

**FINAL REPORT OF THE NKFIH FK 124807 PROJECT**  
**GEOCHRONOLOGY OF GLACIAL LANDFORMS AND CAVE SEDIMENTS IN MACEDONIA AND**  
**IMPLICATIONS FOR QUATERNARY LANDSCAPE EVOLUTION**  
**IN THE CENTRAL BALKAN PENINSULA**

Principal investigator: Zsófia Ruzsukiczay-Rüdiger.

Participants: Marjan Temovski, Zoltán Kern, Balázs Madarász, Ivica Milevski, Mihály Braun.

Aiming at an improved understanding of the Quaternary landscape evolution and paleoclimate of the Central Balkan Peninsula (CPB) the team of this project set up two working packages:

(1) To provide a deglaciation **chronology via exposure age determination** of glacial landforms in several major mountain ranges situated along a ~500 km-long transect across a central diagonal of the Balkan Peninsula from the Jablanica Mts (SW Macedonia) to the Retezat Mts (Romania) (Fig. 1). This work package also aimed at the **reconstruction of the paleo-glaciers** in the studied areas, to calculate their equilibrium line altitudes (ELAs) in order to **derive paleoclimate data** (temperature and precipitation).

(2) To decipher the evolution of the Crna Reka and Radika River basins via **burial age determination of sediments trapped in caves** to **estimate the age of the caves** and based on their relationship to the base level, to **estimate river incision rate/surface uplift rate** following the draining of the Pliocene Macedonian Lake system.

Beside these main objectives, methodologically related studies, including uplift rate quantification within the Pannonian Basin and laboratory inter-comparison project are among the achievements of the project.

## 1. Tracing signs of previous glaciations, exposure age determination of glacial landforms and reconstruction of paleo-glaciers



Fig.1. Mountain ranges where paleo-glacial studies were carried out during the project

Although glacial landforms on the Balkan Peninsula have been studied since the 19th century, only scarce data are available about the extent of the former glaciations in the Central Balkan Peninsula, the transition zone between the Mediterranean and Central Europe. Three target areas were selected for the detailed study of paleo-glaciations of the CBP: The Jablanica, the Jakupica and the Šar Mts. Geomorphological mapping and glacier reconstruction were carried out to demarcate the extent of the former glaciations. Cosmic ray exposure (CRE) dating using in situ produced  $^{10}\text{Be}$  was applied to quantify the age of the glaciations. The spatial parameters and age of the reconstructed glaciers were used to assess the hydroclimate during the glacial phases.

Four peer reviewed studies were published in this topic so far, three of these deal with the glaciations in North Macedonia, related to the work carried out in the Jablanica and Jakupica Mountains. The fourth one is a study from the Retezat Mts, Southern Carpathians, which is an analogous site to the Macedonian high mountains of similar elevation, but more inland and northerly setting (Fig. 1). It was the result of the evaluation of a formerly collected dataset during the COVID19 pandemic, when restrictions on fieldwork and laboratory work hindered the acquisition of new samples and age data. The preliminary morphometric analysis of the cirques in the Šar Mts. was published in a conference proceedings study. Furthermore, two Q1/D1 papers are in preparation based on the geochronological datasets from the Šar Mts that arrived, or are still expected by the end of the timespan of the present project. In the following the published studies are summarised briefly, and the unpublished, ongoing work is presented in more detail.

## PUBLISHED RESULTS

### *1.1. Glacial geomorphology glacier reconstruction and age determination of the subsequent glacial phases in the Jablanica Mt. (North Macedonia)*

Glacial features of the Jablanica Mt. were mapped, described and classified into morphostratigraphic units. According to the new glacio-geomorphological map the glacial landforms were assigned to six morphostratigraphic units. Ten primary and two secondary cirques were identified in the upper parts of the studied valleys, while downstream the valleys were steep and glacially shaped with several glacial steps and thresholds. Cirque and valley morphology indicate that subglacial deepening was limited within the cirques and was more intensive in the valley sections during more extensive glacial phases. The largest reconstructed glaciers were 4.6–7 km long, while the last cirque glaciers had only a few hundred meters length. Using morpho-stratigraphic data, a glacier reconstruction was carried out for the largest mapped glacial extent. On the basis of glacial geomorphology, a former ELA of ~1800 m and glacier cover of 22.6 km<sup>2</sup> were estimated during this stage (Temovski et al, 2018).

In the following study  $^{10}\text{Be}$  cosmic ray exposure (CRE) ages were provided for a succession of glacial landforms in the Jablanica Mt. aiming at a better understanding of the glacier development in the area. On the basis of the mapped glacial landforms six glacial stages were reconstructed and their mean ELAs were estimated using the AABR method (Osmaston, 2005). The CRE ages of five glacial stages - from the second largest to the smallest - were determined between 16.8<sup>+0.8</sup>/<sub>-0.5</sub> ka and 13.0<sup>+0.4</sup>/<sub>-0.9</sub> ka. Accordingly, the most extended glaciation in the Jablanica Mt. occurred before ~17 ka. The average ELA of the glaciers was 1792±18 m asl during the largest ice extent, and 2096±18 m during the last phase of the deglaciation.

The correspondence with independent reconstructions of key drivers of glaciological mass balance suggests that glacial re-advances during the deglaciation were associated to cool summer temperatures before 15 ka (Fig. 2). The last glacial still-stand was apparently a result of a modest drop in summer temperature coupled with an increased winter snow accumulation. In the study area no geomorphological evidence for glacier advance after ~13 ka could be found, most probably because low temperatures were combined with dry winters (Ruszkiczay-Rüdiger et al, 2020a).

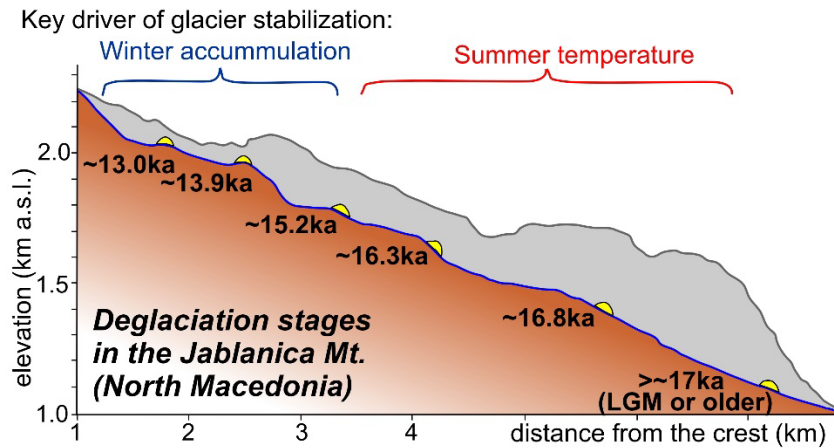


Fig. 2. Age and elevation of moraines of the dated phases of deglaciation and key drivers of the glaciological mass balance in the Jablanica Mt after the LGM (Ruszkiczay-Rüdiger et al, 2020a)

1.2. Glacier chronology and paleoclimate reconstruction in the Jakupica Mt

In the Jakupica Mt. a plateau glacier was reconstructed (max. area ~45 km<sup>2</sup>, max thickness: ~260 m). Detailed mapping and geochronological study targeted six formerly glaciated valleys, five of which were fed by the plateau glacier and one had an independent cirque when local glaciation reached its maximum ice extent (MIE). The ELA of the most extended glacial phase was at 2075<sup>+37</sup>/<sub>-25</sub> m asl. The <sup>10</sup>Be CRE age of this phase was estimated at 19.3<sup>+1.7</sup>/<sub>-1.3</sub> ka, conformable with the LGM. CRE ages from the next moraine generation placed the first phase of deglaciation to 18.2<sup>+1.0</sup>/<sub>-3.0</sub> ka. The samples from the moraine of the penultimate deglaciation phase provided CRE ages with large scatter and biased towards old ages, which is probably the result of inherited cosmogenic nuclide concentrations within the rock (Fig. 3).

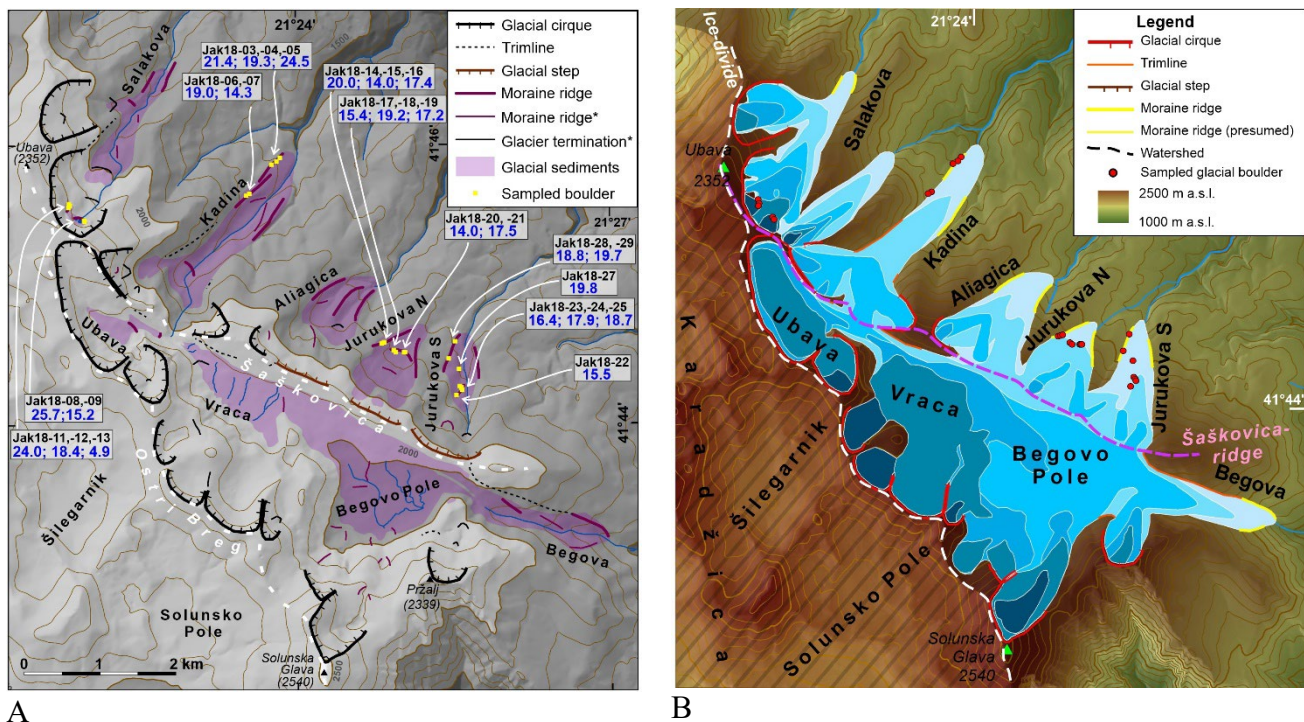


Fig. 3. Results of geomorphological mapping and CRE dating (A) and glacier reconstruction (B) in the Jakupica Mts). The sample code (black) and ages (blue, ka) appear in boxes in inset A. The reconstructed glacier stages appear in blue, with darker hue towards younger ages on inset B (Ruszkiczay-Rüdiger et al, 2022).

Glacio-climatological modelling was performed for the MIE paleoglaciers, which has a well-established LGM age. The degree-day model was used to calculate the amount of accumulation required to sustain the glaciological equilibrium assuming a certain temperature drop at the ELA for the most extended stage.

Pollen-based paleoclimate reconstructions used for the glaciological modelling suggest a mean annual temperature drop of 5°C and increased annual temperature range for the LGM. Using these parameters, the modelled annual total melt at the LGM ELA implies much wetter conditions than today. Alternatively, the model can be constrained with the current annual temperature range and the regional estimates of LGM temperature drop at 6-7 °C. This results in a simulated precipitation that is 1.3 to 1.8 times higher than today. These wetter LGM conditions inferred from the paleo-glaciological evidence in Jakupica Mt. suggest an enhanced moisture advection in the region (Ruszkiczay-Rüdiger et al, 2022).

### ***1.3. Glacier chronology and quantification of cosmogenic nuclide inheritance and the depth of glacial erosion in the Retezat Mts, Romania***

When studying glacial landforms, the presence of cosmogenic nuclide concentrations inherited from previous exposure(s) may hinder the determination of their age. Inheritance is indicative of limited glacial erosion or of a complex exposure history, and this might, in turn, be revealed by a bias towards older ages in apparent exposure durations.

A dataset of 45 samples for  $^{10}\text{Be}$  CRE dating was used to set up the deglaciation chronology in the southern valleys of the Retezat Mts. The samples from the cirque area permitted the quantification of a considerable amount of inherited  $^{10}\text{Be}$  in the glacial boulders and bedrock samples. The samples from the glacial phases of the largest glacier extent display no signs of significant inheritance, thence enabled the establishment of a deglaciation chronology. The timing of the maximum glacier extent ( $20.6^{+0.8}_{-1.3}$  ka) coincided with the LGM, which was followed by five deglaciation phases during the Lateglacial (at  $18.4^{+0.7}_{-1.1}$  ka;  $16.9\pm 0.9$  ka,  $15.8^{+0.9}_{-0.6}$  ka,  $15.6^{+0.8}_{-0.8}$  ka and  $14.4\pm 0.5$  ka).

Given the lack of independent geochronological data, the amount of inherited cosmogenic nuclides is tentatively estimated by accepting the youngest cosmic ray exposure age(s) as the time of moraine deposition and abandonment by the glacier. The calculated amount of inherited  $^{10}\text{Be}$  enables the estimation of a glacial erosion depth of 1.1–1.4 m for the bedrock samples and 1.4–1.7 m for the glacial boulders (Fig. 4). The duration of the ice-covered and ice-free periods was adjusted in relation to independent paleoenvironmental and paleoclimatological data. The glacial denudation rate in the cirques was estimated at 20-24 mm/kyr and 25-29 mm/kyr for bedrock and boulders, respectively.

The limited glacial erosion in the cirques is attributed to frozen-bed conditions with no considerable glacial deepening during the more extended glacial phases. Only when warming led to the retreat of the glaciers to their cirques, they become steeper and shift to being warm-based and thus more erosive. However, the limited time spent under these conditions appears to be too short to remove material from the cirque floors in sufficient depth (>3 m) to reset the cosmogenic clock.

Considering the well developed glacial landscape observed in the Retezat Mts, coupled with the limited glacial erosion during the LGM suggested by the CRN inventories of the landforms of the cirque area, implies that glacial landscape of the Retezat Mts must have been formed in the course of at least two, or possibly more glacial phases. In the absence of numerical ages for glacial landforms older than LGM, this is the first evidence of pre-LGM glaciation of the Southern Carpathians.

The currently available geochronological data do not support the assumption of any major glacial re-advance after Greenland Stadial 2a (GS-2.1a, end of Pleniglacial) in the Retezat Mts (Ruszkiczay-Rüdiger et al, 2021).

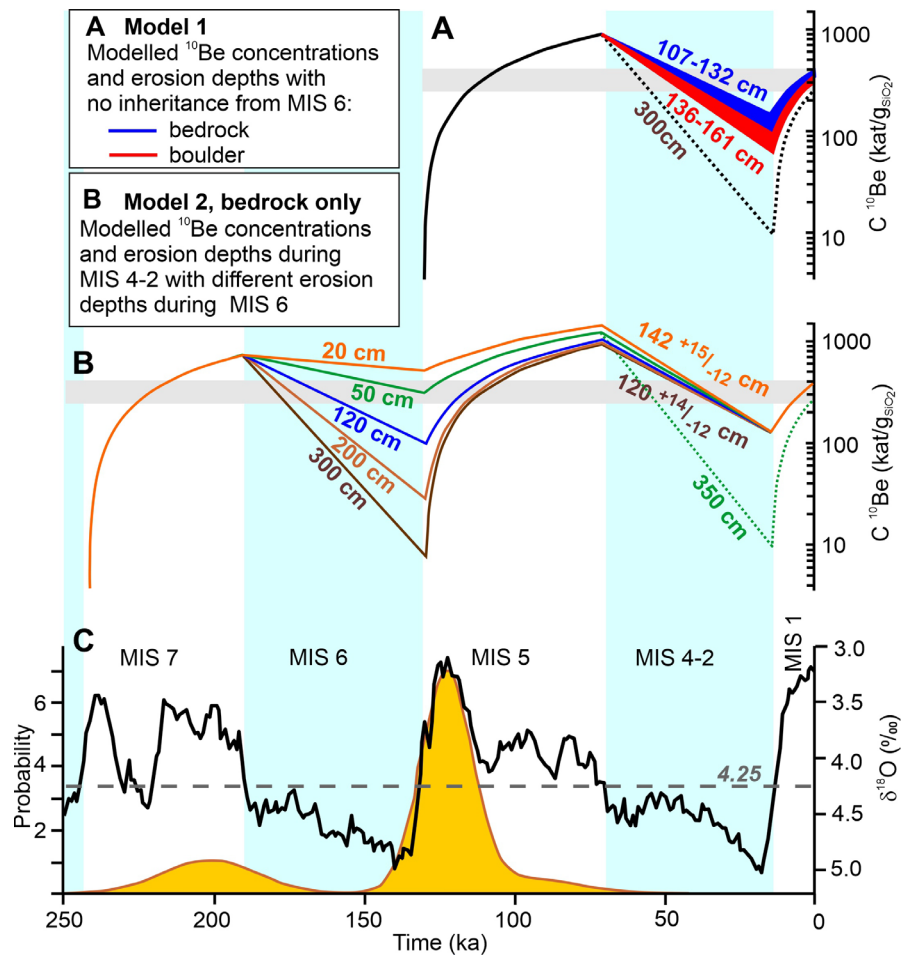


Fig. 4. Modelled evolution of  $^{10}\text{Be}$  concentrations over time in the Berbecilor Cirque. A: Considering the last glacial cycle and no inheritance from the penultimate glaciation. B: Considering the last two glacial cycles. The brown lines indicate the 300 cm denudation depth, which is deep enough to reduce the inherited  $^{10}\text{Be}$  inventory below detection limit. C: The benthic  $\delta^{18}\text{O}$  record and Marine Isotope Stages and kernel density estimate of speleothem U-Th age data from alpine caves in the Făgăraș Mts (Tîrlă et al., 2020; orange plot). The grey dashed line shows the  $\delta^{18}\text{O}$  value of 4.25 ‰, which best fits both the U-Th speleothem data and the MIS stages and used as a threshold value to estimate the duration of unglaciated and glacier-covered periods in the study area (light blue shadows) (Ruszkiczay-Rüdiger et al, 2021).

#### 1.4. The Geomorphometry of the cirques in the Šar Mountains

As a basis of the recognition of the significance of paleo-glaciations in the Šar Mts, cirque landforms were identified and mapped. The distribution of the cirques was completed with an analysis of their quantitative features. Aside from fieldwork, nowadays this can be accomplished through analysis of digital terrain models. Based on the very detailed 5-m DEM and 0.5-m orthophoto imagery, 55 glacial cirques were identified on the North Macedonian side of Šar Mountains, and their shape, size, height, slope, and dominant aspect were calculated. Most of the cirques are located between 2100 m and 2500 m a.s.l., and have E, N and NE aspects, steep headwalls and almost flat floors. There is a difference in the altitude and size of the cirques considering their general aspect and overall position (Milevski et al, 2020).

## STUDIES IN PREPARATION

### 1.5. *Glacier reconstruction and chronology of the Šar Mts. and paleoclimate implications*

Fieldwork, sample processing and isotope measurements were hindered for the Šar Mts, the third study location of the glacial research of our project in North Macedonia. The last measurement results were completed only during the summer of 2023, and their interpretation is on its way.

Two manuscripts are in preparation:

The first one will provide geomorphological mapping and  $^{10}\text{Be}$  CRE geochronological results and will quantify the extent and timing of the most extensive glaciation. On this basis the glacier will be reconstructed and ELAs will be calculated, enabling to model the humidity conditions relevant for this phase.

The second one is planned to deal with the subsequent shrinking of the glaciers and the age of the final deglaciation of the area. It will also be dedicated to explain the apparently controversial CRE ages and the possible role of inherited cosmogenic  $^{10}\text{Be}$  inventories, and the possibilities of the calculation of the depth of glacial erosion in the presence of an independent age constrain by adding  $^{14}\text{C}$  CRE ages data to certain samples.

In the following the study objectives, methods, results and preliminary interpretations are described in brief.

#### 1.5.1. *Introduction and objectives*

The Šar Mts are located in the NW boundary of North Macedonia. Considerable part of this range is above 2000 m asl elevation with its highest peak above 2700 m asl (Titov Vrv, 2747 m). Its valleys have a well-expressed glacial morphology with cirques in variable state of development (Milevski et al., 2020). However, there is limited data about the age of the glaciations and the climate conditions necessary for the glaciation of this mountain range (Kuhleemann et al., 2009; Menković and Milivojević, 2021).

The objective of our study was to constrain the size and age of the glaciers starting from the most extended glaciation, then to reconstruct the subsequent shrinking of the glaciers through mapping the glacial landforms. Next step is the age determination of the landforms created during the still-stands or smaller pushes of the melting glaciers.

The mapped landforms and new numerical ages will allow us to reconstruct the formerly existing glaciers, and to calculate their ELAs for several deglaciation phases. In the presence of an independent estimate of the paleo-temperatures at the former ELA, it is possible to calculate the amount of mean annual snowfall to sustain the glaciers in equilibrium.

#### 1.5.2. *Methods*

Mapping of the glacial landforms followed the protocol described in Ruzkiczay-Rüdiger et al. (2022). The glacial chronology was set up by  $^{10}\text{Be}$  CRE dating. The sampling strategy, laboratory methods and age calculations occurred as described in Ruzkiczay-Rüdiger et al., 2021a and 2022).

The Accelerator Mass Spectrometry (AMS) measurements of the  $^{10}\text{Be}/^9\text{Be}$  ratios of the samples were completed at Vienna Environmental Research Accelerator, Department of Isotope Physics, University of Vienna (VERA) financed by independent proposals for the access of AMS beam-time hours (RADIATE Transnational Access project grants 20002322-ST and 22002978-ST).

The first sample set was collected in the Bozino, Idrizova Dupka, Skakalo and Dobrošte valleys in 2019 (n=36). A second set was collected in the Skakalo2, Karanikolica and Kazanište valleys in 2021 (n=33) (Figs. 5, 6, 7, 8). In 2020 it was not possible to do fieldwork due to the COVID restrictions.

The processing and AMS measurement of the 1<sup>st</sup> sample set was hindered by the close up due to the pandemic and the measurement results arrived by the end of 2021. The 2<sup>nd</sup> sample set was processed during 2022 and due to a breakdown of the accelerator at VERA, the AMS measurements of the  $^{10}\text{Be}/^9\text{Be}$  ratios were completed only in July in 2023, after the closing of the project.

In the following the preliminary interpretation of this large dataset (n=69) is presented. The ages might be subject of minor changes yet, and for simplicity in the text their most probable values are used. The internal

uncertainties of the data are usually around 3-5%, and the external uncertainties are mostly ~9-10%. The calculated ages and their internal uncertainties appear in Figs. 6, 7, 8)

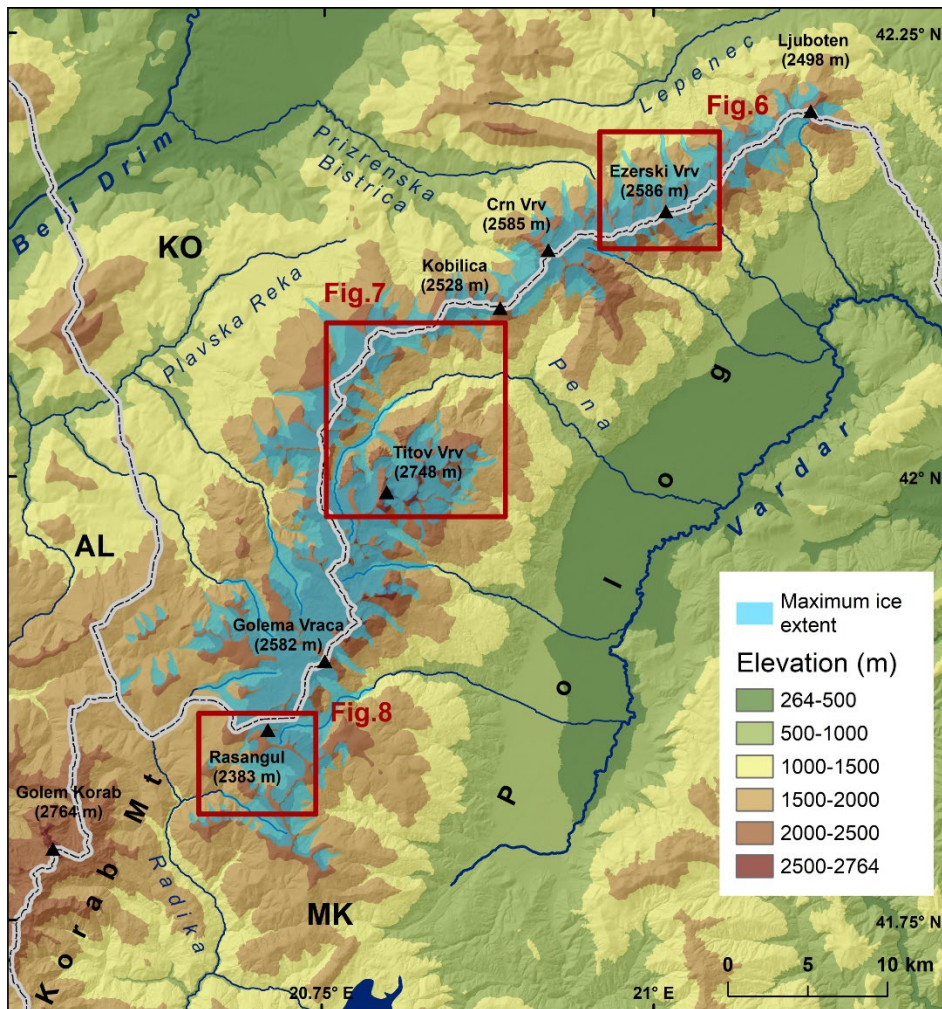


Fig. 5. Digital elevation model of the Šar Mts. with the maximum ice extent reconstructed using the topographic maps, geological map, DEM and GoogleEarth imagery together with published glacier reconstructions (Kuhlemann et al, 2009 and Menković and Milivojević, 2021). Red rectangles indicate the position of the studied areas shown in Figs 6, 7, 8.

### 1.5.3. Results

The novel CRE ages are quite consistent with the morpho-stratigraphic position of the samples at certain valleys, while providing confusing pattern in other settings.

In the northern area, in the Dobrošte valley, the largest mapped glaciation extended down to ~1880 m asl and  $^{10}\text{Be}$  CRE data ( $n=14$ ) suggest that it occurred in the LGM. However, the age of the samples taken from the moraine of the second smallest glacier (~2260 m asl) was inconsistent and apparently too old: ~17.8 ka and ~36.6 ka (Fig. 6A). The CRE data published by Kuhlemann et al. (2009) were recalculated in order to make consistent comparison with the current dataset. These show a large scatter for the most extended phase, with one out of three samples in agreement with the LGM age, supporting the interpretation of the original work. In the cirque areas the recalculated CRE ages were of 15-13 ka (Fig. 6).

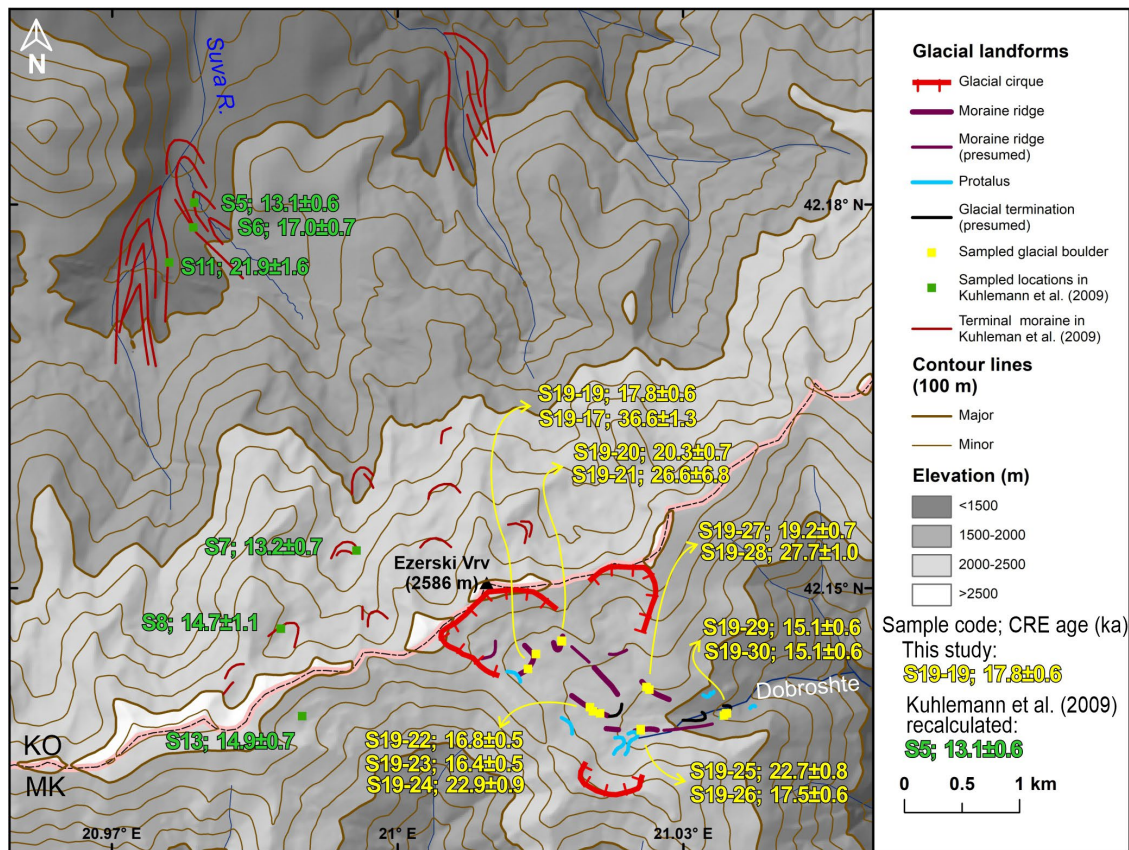


Fig. 6. Digital elevation model of the study area in the northeastern part of the Šar Mts (Dobrošće valley) with the geomorphological map, sample locations and calculated  $^{10}\text{Be}$  CRE ages. The sample locations of Kuhlemann et al (2009) are included, with recalculated  $^{10}\text{Be}$  ages.

In the central part of the range four valleys were studied (Fig. 7). The largest glaciers terminated around 1560 m asl. The obtained CRE ages ( $n=38$ ) suggest that the most extended glaciation occurred during the LGM (Skakalo valley), and was subject of a considerable periglacial reworking until ~17-18 ka (Skakalo, Skakalo2). In the Karanikolica valley the CRE data are difficult to interpret. Here the samples taken from the moraine of the most extended glacier yielded  $^{10}\text{Be}$  ages between ~16.2 and ~4.1 ka, being too young compared to their morpho-stratigraphic position. In the Kazanište valley no sample could be taken from the largest phase.

The moraines of the subsequent deglaciation phase were well expressed in the Skakalo2 valley, extending down to 1950-2050 m asl. Their  $^{10}\text{Be}$  age is ~14-16 ka.

Moraine deposits belonging to the cirque glaciation were dated in the Karanikolica (~2200 m asl), Skakalo2 (2230 m) and Kazanište valleys (~2180 m), yielding CRE ages of ~17.1-18.3 ka, ~12.0-14.5 ka and ~13.3-15.1 ka, respectively. The  $^{10}\text{Be}$  ages of the Karanikolica valley were in very good agreement with each other and also with the recalculated age of the sample of Kuhlemann et al. (2009), however, they point to a considerably older age, ~17-18 ka, respective to the position of the landform.

In the Kazanište valley the moraine or moraine-protalus complex of a glacieret extending down to 2320-2340 m asl. was dated to ~10.6-9.0 ka. This might be the age of the last ice patches in the range, where the high elevation and northerly facing cirque walls favoured the late disappearance of the glacier ice.

In the Karanikolica valley two samples from a protalus at ~2310 m asl. yielded a late Holocene age of ~2.1 ka suggesting the presence of a perennial snow patch most probably due to an accumulation-favoring climate spell.



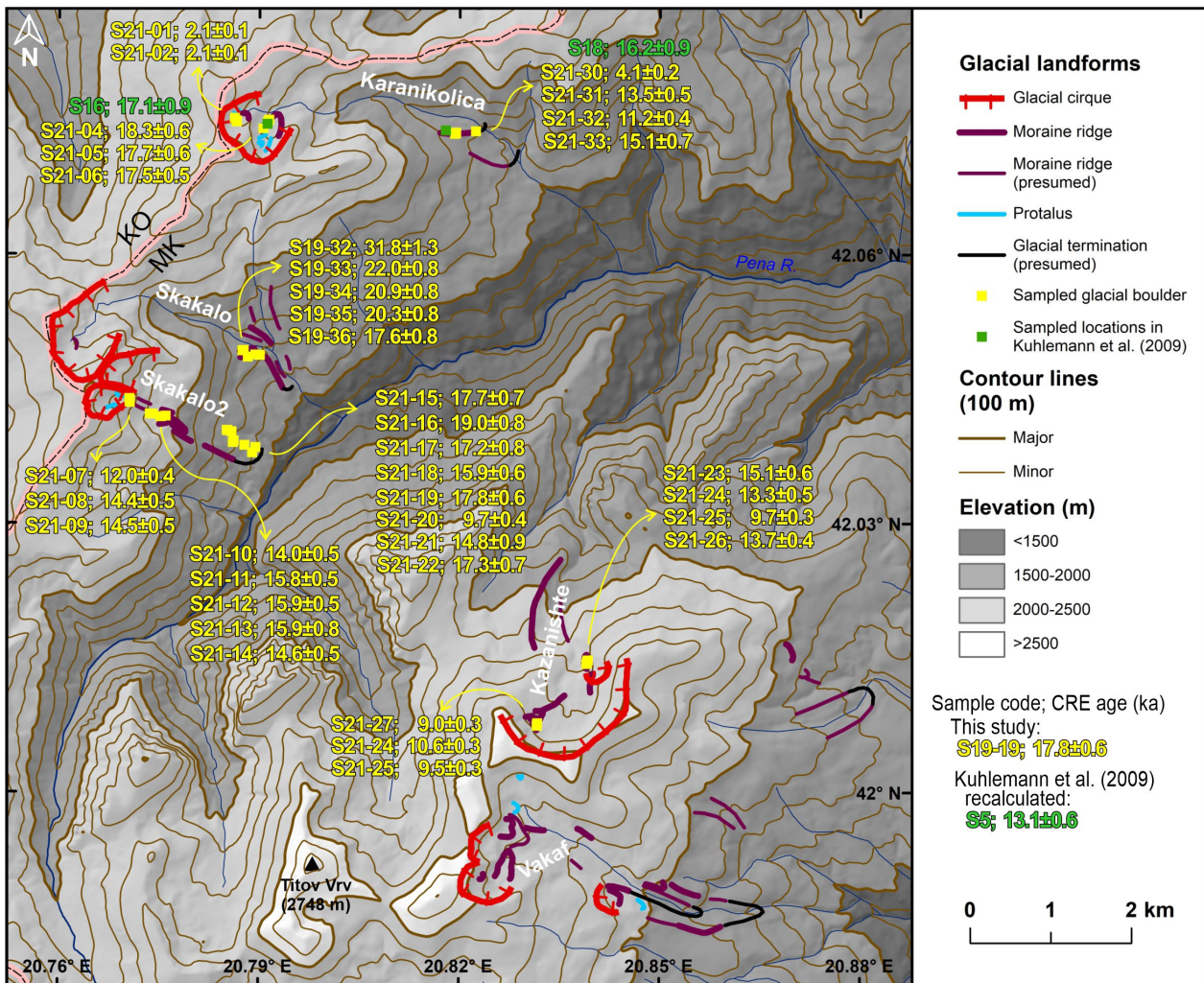


Fig. 7. Digital elevation model of the study area in the central part of the Šar Mts (Karanikolica, Skakalo, Skakalo2 and Kazanište valleys) with the geomorphological map, sample locations and calculated  $^{10}\text{Be}$  surface exposure ages. The sample locations of Kuhlemann et al (2009) are included, with recalculated  $^{10}\text{Be}$  ages.

In the southern part of the Šar Mts two valleys were mapped and sampled ( $n=16$ ) (Fig. 8). The most extended glaciers descended down to  $\sim 1750$  m. The age determination of this phase provided quite controversial results with CRE ages of  $\sim 18.8$ ,  $\sim 31.1$  and  $\sim 49.4$  ka on a lateral moraine in the Idrizova Dupka valley and  $\sim 83.7$  ka and  $\sim 32.5$  ka on the lateral moraine and  $\sim 19.4$  ka on an erratic boulder in the Božino valley.

The age determination of the cirque glaciations provided similarly puzzling results. The moraine of the cirque glacier in the Idrizova Dupka valley at  $\sim 2120$  m, yielded apparent CRE ages of  $\sim 17.4$  ka and  $\sim 19.9$  ka, and in the somewhat lower Božino valley at  $\sim 1950$  m, boulder CRE ages were  $\sim 29.2$  ka,  $\sim 24.2$  ka and  $\sim 14.4$  ka. Close to the cirque walls boulders from protalus ramparts were also sampled resulting in 12.0 ka in Idrizova Dupka ( $\sim 2140$  m asl) and 15.7 and  $\sim 21.7$  ka in Božino ( $\sim 2000$  m asl).

Large scatter of ages in a lateral moraine may suggest the recycling of boulders from a previous stage of similar glacial extent, so that boulders of variable exposure durations are present in the same landform. In valleys, where the estimated exposure durations are very scattered for a single landform and/or do not perform the morpho-stratigraphically predicted trend of younger ages of landforms in subsequently higher position up-valley, the excess of  $^{10}\text{Be}$  concentration in the rocks needs explanation.

The unrealistically old ages in the moraines of the cirque area of some valleys, mostly those with relatively poorly developed, shallow cirques (Božino, Idrizova Dupka) suggest that there was an excess of cosmogenic  $^{10}\text{Be}$  in the rock at the time of deposition (inheritance), which makes the apparent exposure ages older than the real time of deposition. Similar phenomenon was described in our study area in the Southern Carpathians,

the Retezat Mts (Ruszkiczay-Rüdiger et al., 2021b) and in the Jakupica Mts, in North Macedonia (Ruszkiczay-Rüdiger et al., 2022)

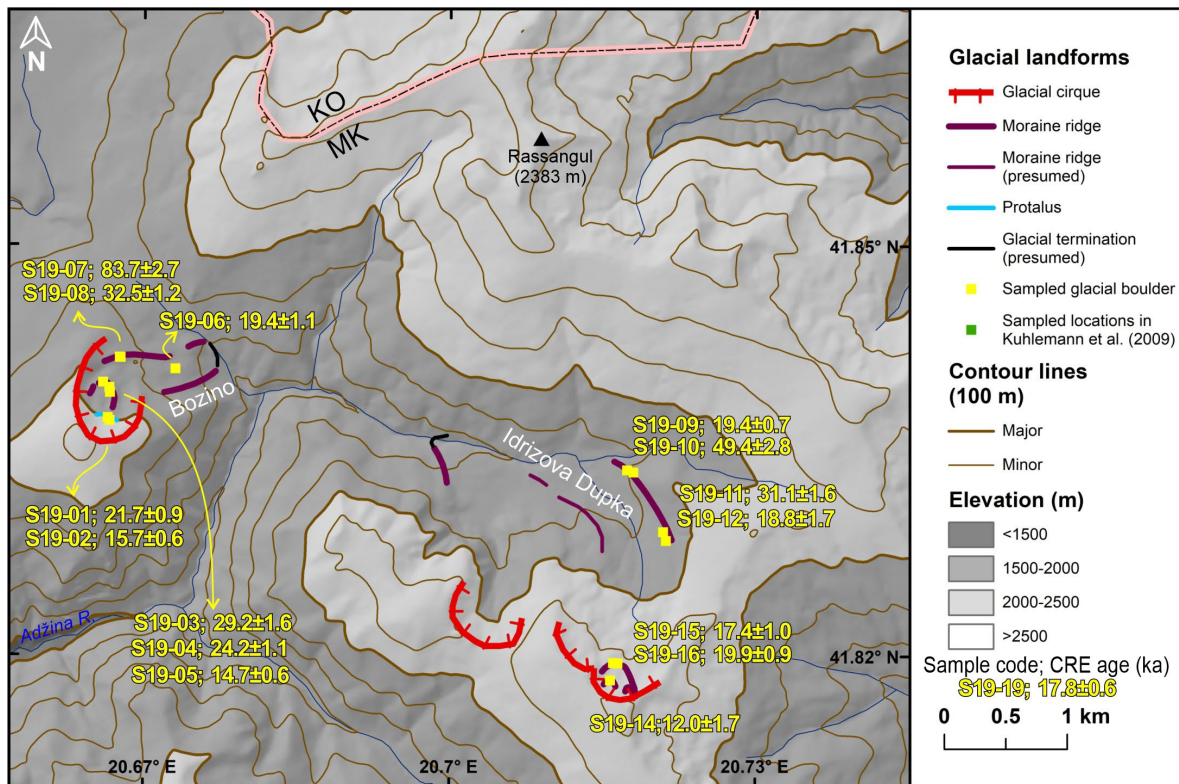


Fig. 8. Digital elevation model of the study area in the southern part of the Šar Mts (Božino and Idrizova Dupka valleys) with the geomorphological map, sample locations and calculated  $^{10}\text{Be}$  surface exposure ages.

In order to better constrain the age of the last glacial phases and the amount of inherited  $^{10}\text{Be}$  in the rocks an independent age determination is necessary. The measurement of the cosmogenic in situ produced  $^{14}\text{C}$  is a plausible solution for two main reasons: Firstly,  $^{14}\text{C}$  is produced and preserved in the crystal lattice of quartz, similarly to  $^{10}\text{Be}$ , therefore it can be measured from the purified quartz obtained from the samples collected for the  $^{10}\text{Be}$  measurements, if there is enough sample material. Secondly, its short half-life prevents it from preserving exposure prior to the LGM, thence even if there were inherited  $^{14}\text{C}$  nuclides after the previous glacial phases these inventories have already decayed, and the measured  $^{14}\text{C}$  concentrations should reflect the amount accumulated only after the last deglaciation.

Therefore, following the puzzling  $^{10}\text{Be}$  results of the first sampling campaign, a RADIATE Transnational Access proposal was submitted in early 2023 for the measurement of the in situ  $^{14}\text{C}$  content of 9 selected samples at the ETH, Laboratory of Ion Beam Physics, Zurich. The proposal gained support (23003128-ST) and the extraction of carbon from the quartz was successfully completed during the summer. The AMS measurement results are expected in the autumn of 2023. The new  $^{14}\text{C}$  data is expected to make the chronology of the latest glacial phases more robust. Besides, the independent age data will enable the quantification of the inherited  $^{10}\text{Be}$  in the sampled rocks which is a function of the depth of glacial erosion during the LGM.

The glacier reconstruction work got started with the modelling of the glaciers of maximum ice extent. The first step was a rough estimation for the entire mountain range using the topographic maps, geological map, DEM and GoogleEarth imagery together with published glacier reconstructions of Kuhlemann et al. (2009) and Menković and Milivojević (2021) (Fig.5). The glacier geometry of the ice field and outlet glaciers are reconstructed by the GlaRe, a semi-automated GIS-based method (Pellitero et al., 2016) using the 9 m DEM of the study area (Milevski et al., 2013) for the studied valleys only. According to the preliminary results, most glaciers of the Šar Mts descended down to 1500-1700 m as. Their area was of a few  $\text{km}^2$ , their maximum thickness was  $\sim 160$  m.

The reconstructed glaciers and ice-field are used for the calculation of the former ELAs by means of the ELA Calculation toolbox (Pellitero et al., 2015) and applying the area-altitude balance ratio (AABR 1.6) method (Osmaston, 2005). The first ELA estimates are between ~1900 and ~2200 m asl, which values are higher than in other ranges. This work is in progress, thence improved values are expected for the maximum ice extent. The same scheme will be applied for the subsequent phases of deglaciation.

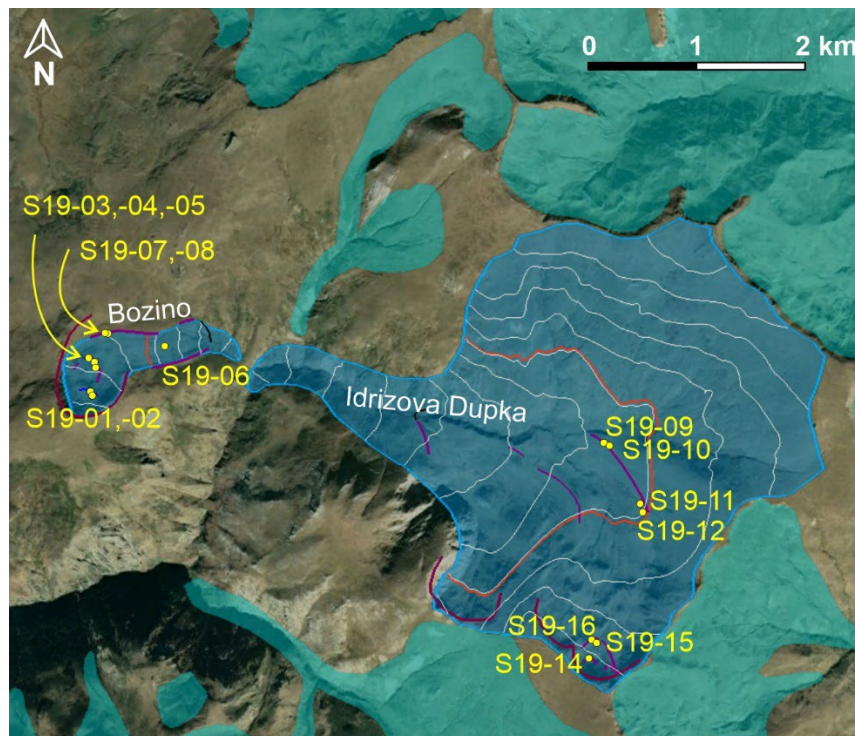


Fig. 9. Maximum ice extent on a GoogleEarth image in the southern part of the Šar Mts with glacial landforms as on Fig. 8. The reconstructed most extended glaciers appear with greenish-blue colour as on Fig. 5. The glaciers appearing in blue with contour lines are the result of the detailed reconstruction in the studied valleys (Božino and Idrizova Dupka). The red lines are the estimated ELAs.

## 2. Cave evolution, chronology and quantification of incision/uplift history

During the project altogether 11 caves were visited and assessed for potential burial age dating using cosmogenic radionuclides (CRN)  $^{10}\text{Be}$  and  $^{26}\text{Al}$  (Fig. 10). In addition to clastic sediments suitable for CRN burial dating, whenever possible, speleothem samples were collected for U-Th dating. Samples were collected from 8 caves, the other caves had no cave deposits suitable for age determination. The relatively large number of sites that proved to be unsuitable and the restrictions due to the COVID19 pandemic resulted in a considerable delay in the laboratory procedures and isotope measurements. Therefore, one manuscript has been submitted and currently it has been re-submitted after moderate revision and two peer reviewed papers are in preparation, as it is described below.

From the sampled caves, burial age was determined from 4 caves (Temna Peštera – Dragožel, Ristea Peštera, Melnička Peštera, Simka Peštera), with samples from two additional caves (Lekovita Voda, Dona Duka) discarded, due to possible presence of autochthonous quartz or not suitable enough material, respectively. For two of the sampled caves (Temna Peštera – Dragožel, Melnička Peštera), a resampling had to be done, due to complicated sample preparations. Additionally, U-Th ages were determined on speleothem samples from 3 caves (Temna Peštera – Dragožel, Liljarnikot, Čulejca).

The obtained geochronological results allow to reconstruct cave and landscape evolution in two drainage systems: Crna Reka, a tributary to Vardar River (draining to the Aegean Sea), and Radika River, a tributary to Crn Drim (draining to the Adriatic Sea). The presentation of the results is organized in three topics. The first one is on the Pleistocene valley incision and tectonic uplift in the lower parts of Crna Reka valley. The

manuscript covering this topic is under the second submission phase being the revised version submitted after moderate revision. The second topic is on the Pliocene-Early Pleistocene landscape evolution in the middle and upper parts of Crna Reka. The third one is on the Pleistocene evolution of Simka Cave, located in the drainage area of the Crn Drim. These manuscripts are in preparation.

For the cave descriptions previously existing maps were revised and completed by field observations and cave mapping. For the  $^{26}\text{Al}/^{10}\text{Be}$  CRN burial dating allocthonous quartz containing sediments trapped in inactive cave galleries could be used. The sample processing occurred as described in Ruszkiczay-Rüdiger et al. (2021a). The Accelerator Mass Spectrometry (AMS) measurements of the  $^{10}\text{Be}/^9\text{Be}$  and  $^{27}\text{Al}/^{26}\text{Al}$  ratios of the samples were completed at Vienna Environmental Research Accelerator, Department of Isotope Physics, University of Vienna (VERA) in November 2022 financed by independent proposal for the access of AMS beam-time hours (RADIATE Transnational Access project grant 22002703-ST).

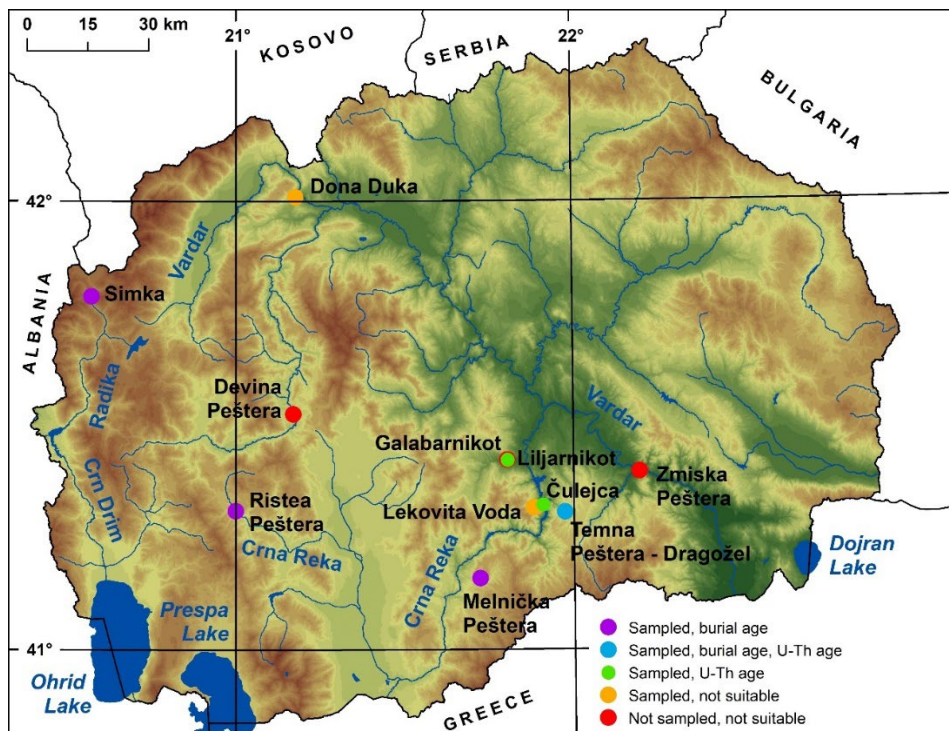


Fig. 10. Location of the studied caves in N. Macedonia.

SUBMITTED, UNDER REVISION

### ***2.1. Pleistocene valley incision, landscape evolution and inferred tectonic uplift in the central part of the Balkan Peninsula – insights from the geochronology of cave deposits in the lower part of Crna Reka basin (N. Macedonia)***

Although the general geomorphology is reasonably well understood, not much information is available on the incision rates of rivers and related tectonic uplift in the central part of the Balkan Peninsula. Caves in the lower part of Crna Reka drainage (N. Macedonia) provide the possibility to reconstruct the Neogene-Quaternary evolution of this area. Previous research has identified two major cave development phases: one related to Pliocene-Early Pleistocene basin fill-up and establishing of lacustrine environments, and a subsequent cave development phase related to valley incision due to draining of the lacustrine systems and tectonic uplift.

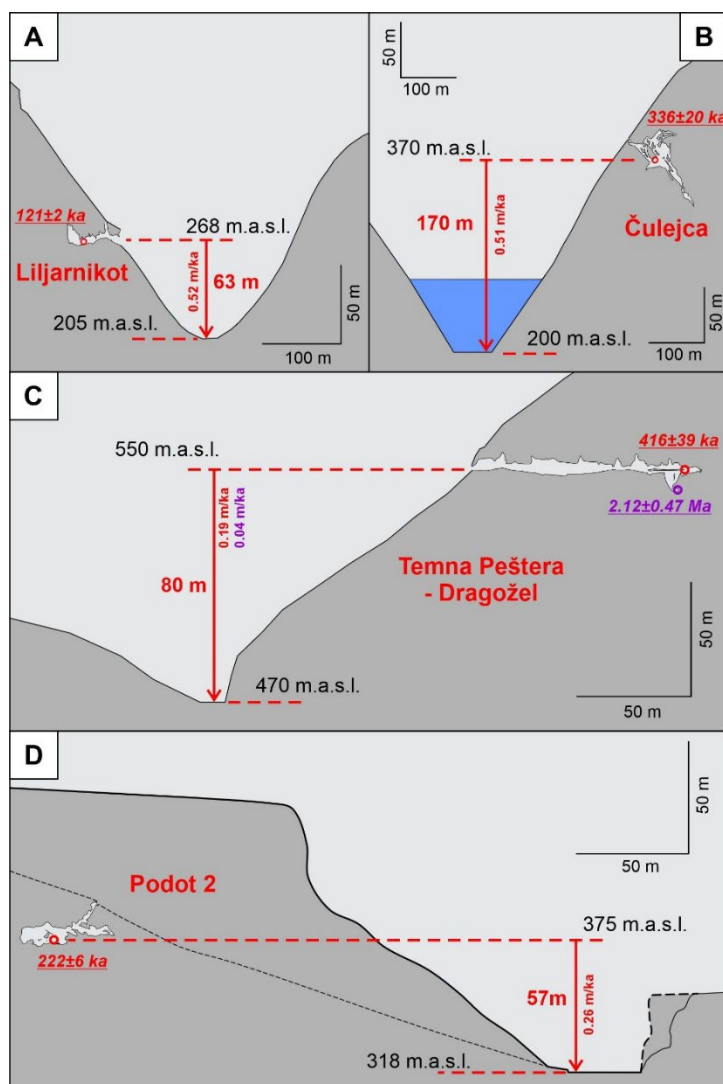


Fig. 11 Cross-sections of the studied caves showing their altitudinal relationship to the current riverbed and calculated valley incision rates based on the obtained geochronological data from the cave deposits. A – Liljarnikot Cave above Raec River; B – Čulejca Cave above Crna Reka; C – Temna Peštera – Dragožel above Kamenica River; D – Podot 2 Cave above Crna Reka. Circles indicate sample location. Red: U-Th dating, purple: CRN burial age dating (Temovski et al, in revision).

New geochronological data were obtained by U-Th dating on speleothems in four caves lying 57 to 170 m above the current riverbed (Liljarnikot, Culejca, Temna Peštera – Dragožel and Podot 2) and CRN burial age determination of allocthonous clastic cave sediments in one cave (Temna Peštera – Dragožel). These data provide time constraints on the Pleistocene valley evolution, and an insight into the related tectonic uplift (Fig. 11). The CRN burial age of fine sand in a sump in Temna Peštera – Dragožel suggests that fluvial sedimentation in the cave lasted until  $2.1 \pm 0.5$  Ma. The cessation of fluvial deposition after this date supports previous results on placing the onset of the draining of the Pliocene lakes in Macedonia in Early Pleistocene. The U-Th age of subaerial speleothem formation (dripstones, flowstones; Liljarnikot, Culejca, Temna) and of mammillary calcites forming in phreatic cave passages (Podot 2) provided an estimate of the karstwater-table lowering related to valley incision (Figs. 11 and 12).

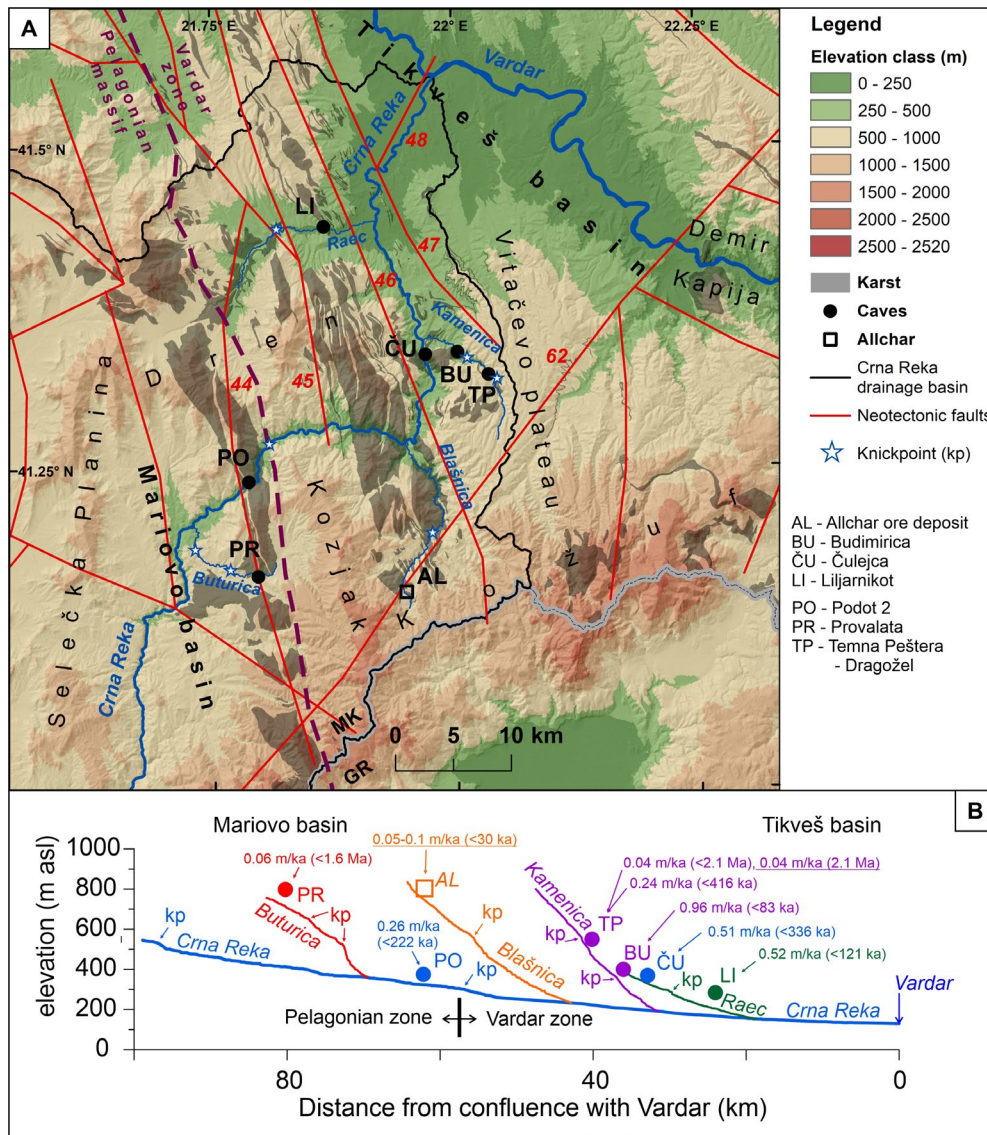


Fig. 12. River drainage in the lower part of Crna Reka basin. A – location where valley incision rate estimates are available (AL: Pavićević at al., 2016; BU: Temovski et al., 2016). Neotectonic faults are from Arsovski (1997). Weakly seismogenic faults are marked with numbers. B – Longitudinal profiles of the Crna Reka and its tributaries in the study area, with the estimated average incision rates. Coloring reflects corresponding valleys. kp: knickpoint (Temovski et al., in revision).

The similar timing obtained along the studied section of the Crna Reka catchment suggests that the draining was more likely initiated by regional uplift, rather than headward erosion related to subsidence in the Aegean Sea. The Middle to Late Pleistocene age of the dated speleothems agrees well with the conceptual model for karst and landscape evolution in the area. The cumulative valley incision rates based on these radiometric data show an increase towards the present, with values of less than 0.1 m/ka in Early Pleistocene, increasing to ~0.2-0.5 m/ka in Middle Pleistocene, and up to 1 m/ka in Late Pleistocene.

Higher uplift rates are inferred for the downstream part of Crna Reka, an area in the Vardar zone bounded by seismogenic faults, than in the upstream part, at the easternmost edge of the Pelagonian massif. The estimated incision rates are lower than recent uplift rates in the area estimated by geodetic levelling (1.1-1.2 m/ka, Lilienberg, 1968), and mostly overlap with the range of GPS-based vertical deformation rates in the Hellenides (0.5-1.0 m/ka; Serpelloni et al., 2022).

STUDIES IN PREPARATION

2.2. Pliocene-Early Pleistocene landscape evolution in the middle and upper parts of Crna Reka drainage (N. Macedonia) unravelled by <sup>26</sup>Al/<sup>10</sup>Be burial dating

Two caves were studied for a better understanding of the Pliocene-Early Pleistocene landscape evolution in the middle and upper parts of Crna Reka catchment: the Melnička Peštera located in Buturica Valley, a tributary to Crna Reka in the middle part of its drainage, and the Ristea Peštera in the upstream part of Crna Reka drainage (Fig. 10).

**Ristea Peštera** is located on the right side of Crna Reka valley, ~100 m downstream from the lowest of the karst springs which represent the actual source of Crna Reka (~734 m asl) The cave entrance is at ~748 m, approximately 20 m above the river bed. The cave has developed in Paleozoic calcite marble and has a general WSW-ENE direction, composed of slightly meandering, phreatic/paragenetic passages in two levels (Fig. 13). The upper level is clogged with sediments, mostly coarse grained, calcite cemented sand. This plug was subsequently eroded so that now there is a narrowing passage continuing downward. A small incision channel in the inner part has developed due to a late vadose stage, which also contributed to the outwashing of cave sediments. A sample of the clastic sediments in the inner part was collected for CRN burial age determination (Fig.13).

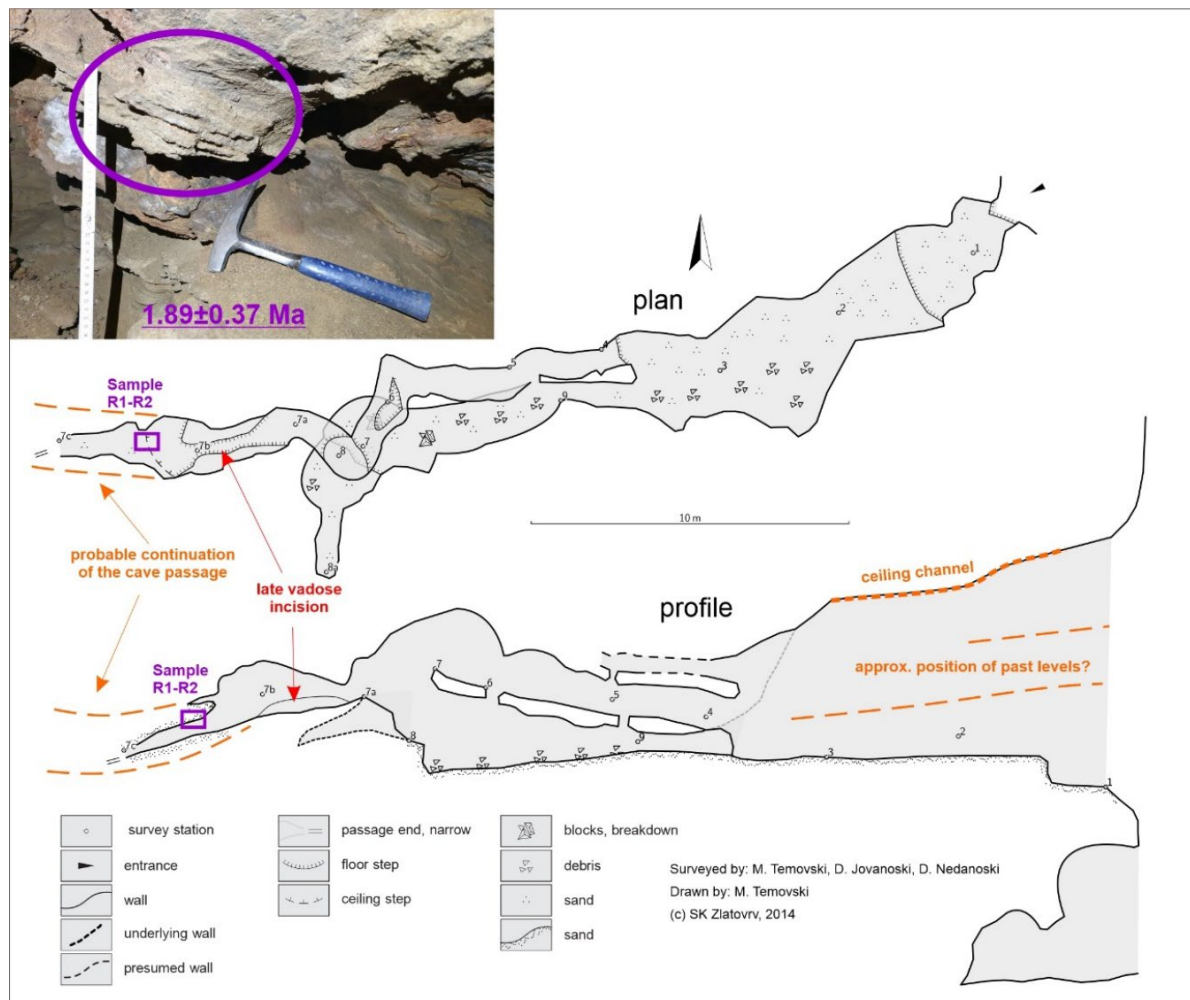


Fig. 13. Detailed cave map of Ristea Peštera with a view of the sampling location.

Considering the wider area, the general discrepancy between the direction of the current drainage (towards SE) and the direction of the valleys generally to the NE and N towards the Cersko karst polje (Fig. 14) it is likely that around this area a drainage capture occurred, diverting the drainage that previously fed the karst

systems to the north, towards the SE oriented drainage of Crna Reka. Subsequently, Crna Reka incised a valley that cut through the previously formed cave systems. Remnants of caves cut by the current valley of Crna Reka are found also upstream from Ristea Peštera. The CRN burial age of  $1.89 \pm 0.37$  Ma, obtained from the clastic sediments in Ristea Peštera, indicates that the NE oriented karst drainage was active in Early Pleistocene and the drainage capture occurred somewhat later.

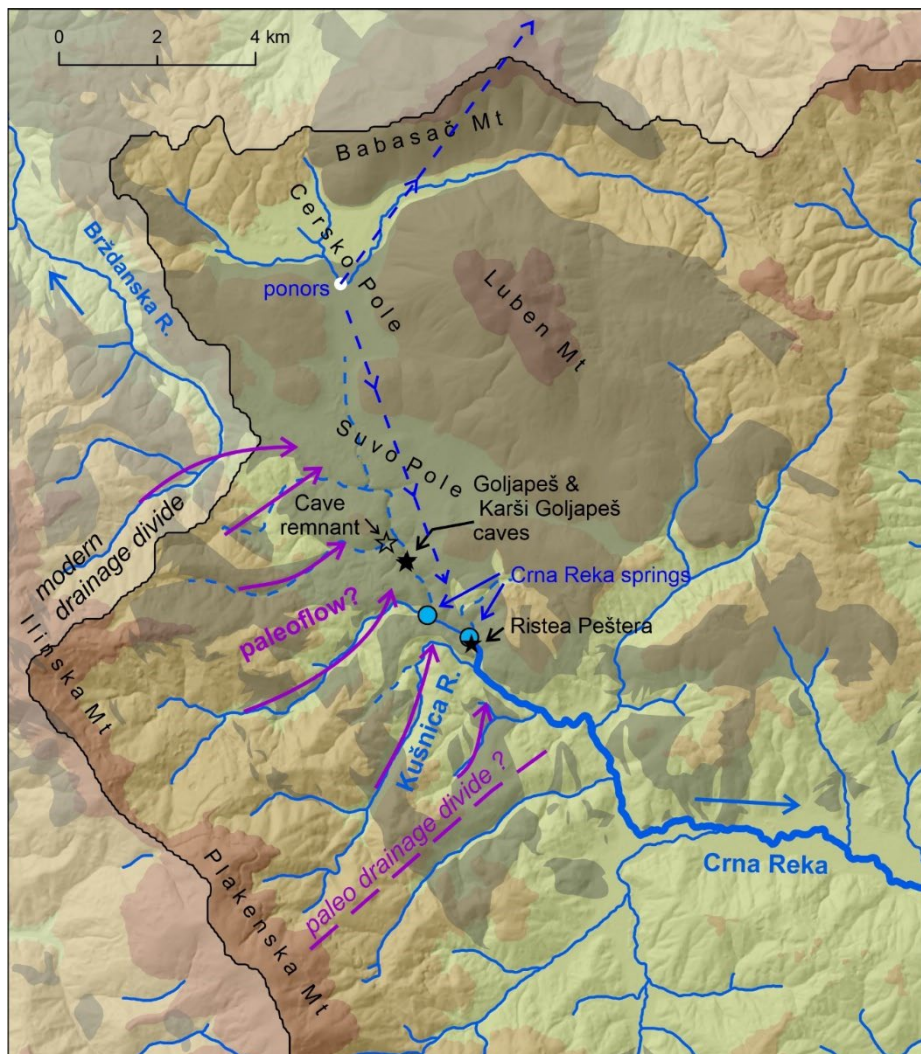


Fig. 14. Geomorphological interpretation of a paleo drainage in the spring area of Crna Reka. Dark shaded areas show the karst terrains.

The **Melnička Peštera** is located in the Pešta Hill, on the right valley side of Buturica valley, a right-hand tributary to Crna Reka (Figs. 10, 15). It is a fossil thermal cave, developed in carbonate breccia deposits composed dominantly of fragments of calcite and dolomite marble with a small percent of non-carbonate rocks such as gneiss, schist and quartz, deposited on top of dolomite marble (Temovski 2016). The material for this breccia was supplied from the north, from the Ramnobor valley (Fig. 15).

This carbonate breccia formation is located at the edge of a basin filled with Upper Miocene to Early Pleistocene sediments, with a hiatus at the end of Miocene (Fig. 15; Dumurdzanov et al. 2004, 2005). The relationship of the breccia to the basin sediments is not clear, due to subsequent erosion or burial. Together with Pliocene fluvial to lacustrine deposits, they form a valley-like depression nested within the Upper Miocene sediments and filled with Pliocene sediments.

This depression is deepening in downstream direction and shallowing in the upstream part, a clear indication of a regression erosion propagation (Fig. 16). A Late Miocene valley incision was identified also further downstream along Crna Reka valley, and has been associated to the base level lowering during the Messinian Salinity Crisis (Temovski 2016; Temovski et al., in revision).



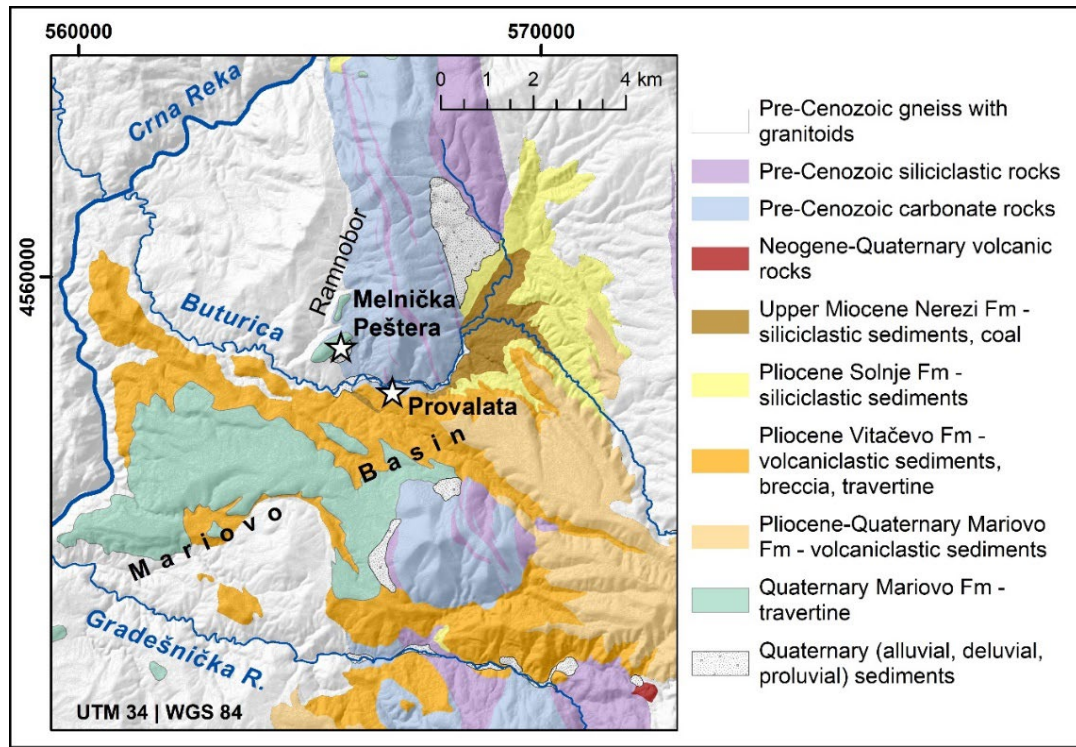


Fig. 15. Geological setting of Melnička Peštera and relationship to Neogene-Quaternary sediments of Mariovo Basin

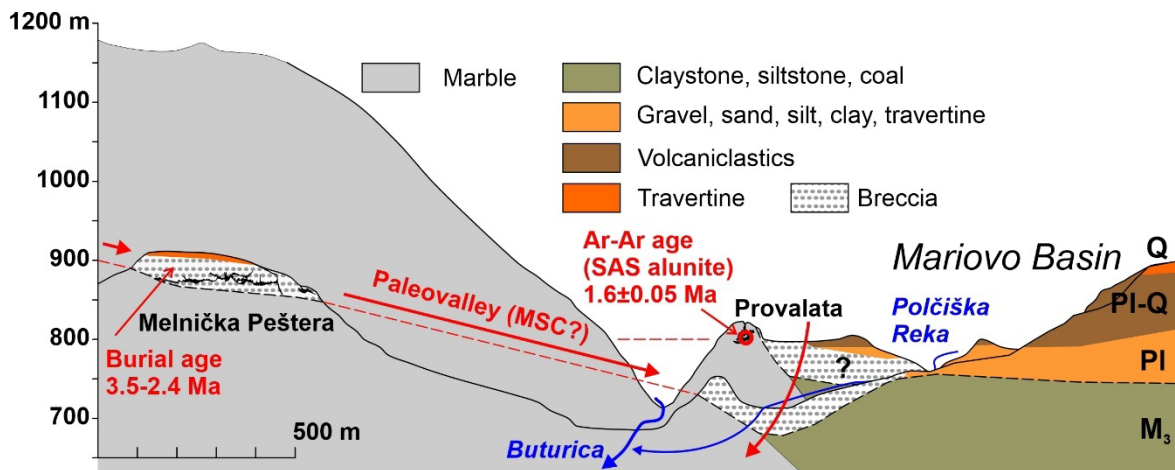


Fig. 16. Composite N-S cross-sections of Melnica area, showing the relationship of the carbonate breccia deposits and other Neogene-Quaternary deposits of Mariovo Basin. Note the incision in the Upper Miocene deposits, filled with breccia deposits.

The mostly horizontal passages of the Melnička cave developed in the carbonate breccia, with the innermost parts formed at the contact of the two formations (Figs 16 and 17). The cave has a hydrothermal origin (Temovski et al. 2022a), similarly to the nearby Provalata Cave, dated to 2.5-1.6 Ma (Temovski et al. 2022b).

The quartz fragments found in the carbonate breccia deposits in the inner part of Melnička Peštera provide a possibility to determine the CRN burial age of this breccia formation, hosting the cave, a peculiar application of the CRN burial dating method. Samples were collected at two locations, close to the contact with the underlying dolomite marble rock. At each location a sample was collected from larger fragments of similar size (M2010-01, M2010-09) and a sample of smaller size fragments (M2010-02; M2010-10). At each sample location the obtained burial ages were overlapping within uncertainty, but with large difference from site to

site (Fig. 17). The ages from the North Passage were  $3.66\pm 0.55$  Ma and  $3.27\pm 0.48$  Ma, and from the Chandelier Room were  $2.17\pm 0.40$  Ma and  $2.60\pm 0.46$  Ma.

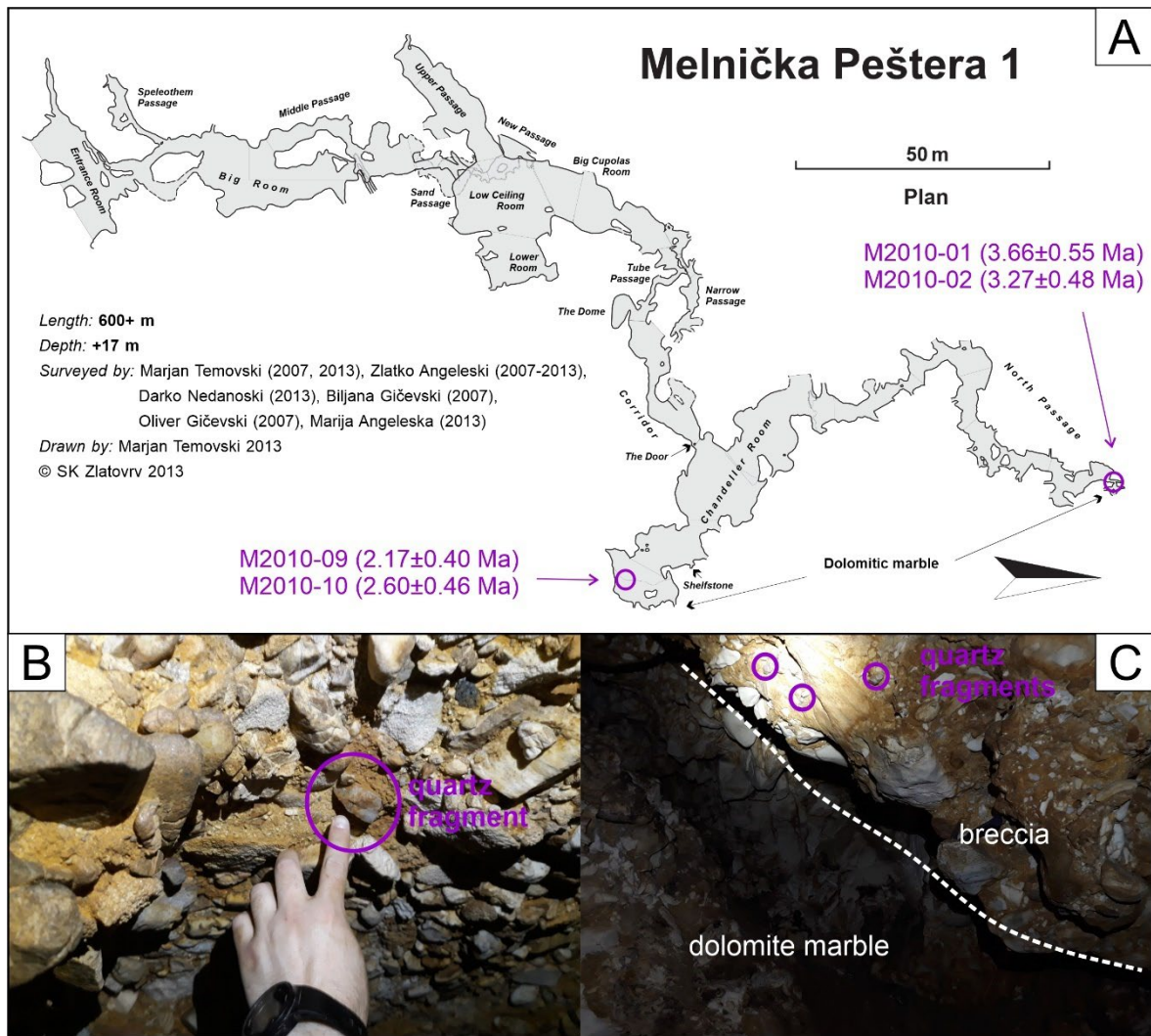


Fig. 17. Location and view of the collected bedrock samples from Melnička Peštera 1. A – location of the sampling sites on the cave map in plan view. B – Close up view of the quartz fragments in the carbonate breccia; C – view of the contact of the carbonate breccia and the underlying dolomite marble rock.

The difference in the grain size of the carbonate breccia deposits in the cave (with presence of large boulders) and the bottom of the valley (generally small size), as well their geometry indicate a fan-like depositional setting. This might explain the difference in the obtained ages that are consistent at a site but showing significant difference between the two locations. This suggest that the fan deposition was active between  $\sim 3.5$  Ma to  $\sim 2.4$  Ma. A minimum age of  $\sim 2.4$  Ma for the deposition of the carbonate rocks is consistent with the supposed timing of the subsequent hydrothermal phase dated between 2.5 and 1.6 Ma in the nearby Provalata Cave (Temovski et al. 2013, 2022b).

Using the new geochronological data and field observations the landscape evolution can be outlined as follows: governed by the deep incision of the paleo-Crna Reka at the end of Miocene, its tributary, the paleo-Buturica was cut also in the Upper Miocene deposits at Melnica. This regressive erosion was likely related to the base level lowering during the Messinian Salinity Crisis. After restoring of the base level, fluvial sedimentation and breccia deposition of variable grain size occurred in a fan-like setting at the junction paleo Buturica and paleo Ramnobor valleys. The breccia formation was topped by travertine deposited mostly in lacustrine environment. The travertines are of thermogene origin (high  $\delta^{13}\text{C}$ ) indicating the onset of hydrothermal activity in the area in Early Pleistocene. The 1.6 Ma age of the sulfuric acid in Provalata Cave (Temovski et al. 2013) reflecting former base level, constrains the subsequent draining of the lake at Melnica and incision of the superimposed valley of Buturica. The incision has drained the hydrothermal Melnička

Peštera that developed within the breccia formation. The cave was eventually decoupled from the hydrothermal system and the subsequent incision during the Pleistocene also led to the removal of large part of the breccia deposits in the middle of the valley.

**2.3. Burial age dating of clastic sediments from Simka Cave, Radika Valley (N. Macedonia)**

Simka Cave is located on the right valley side in the upstream part of Radika River, just before the confluence with its right-hand tributary Štirovica (Fig. 18). The area is along the junction of the Korab Mt to the SW and the Šar Mts to the NE. It was first described by Andonovski (1984), associating its development to an underground stream and attributing a Pleistocene age. New detailed mapping of the cave was done during the present project and samples were collected from a clastic sediment profile for CRN burial age dating (Figs 18 and 19).

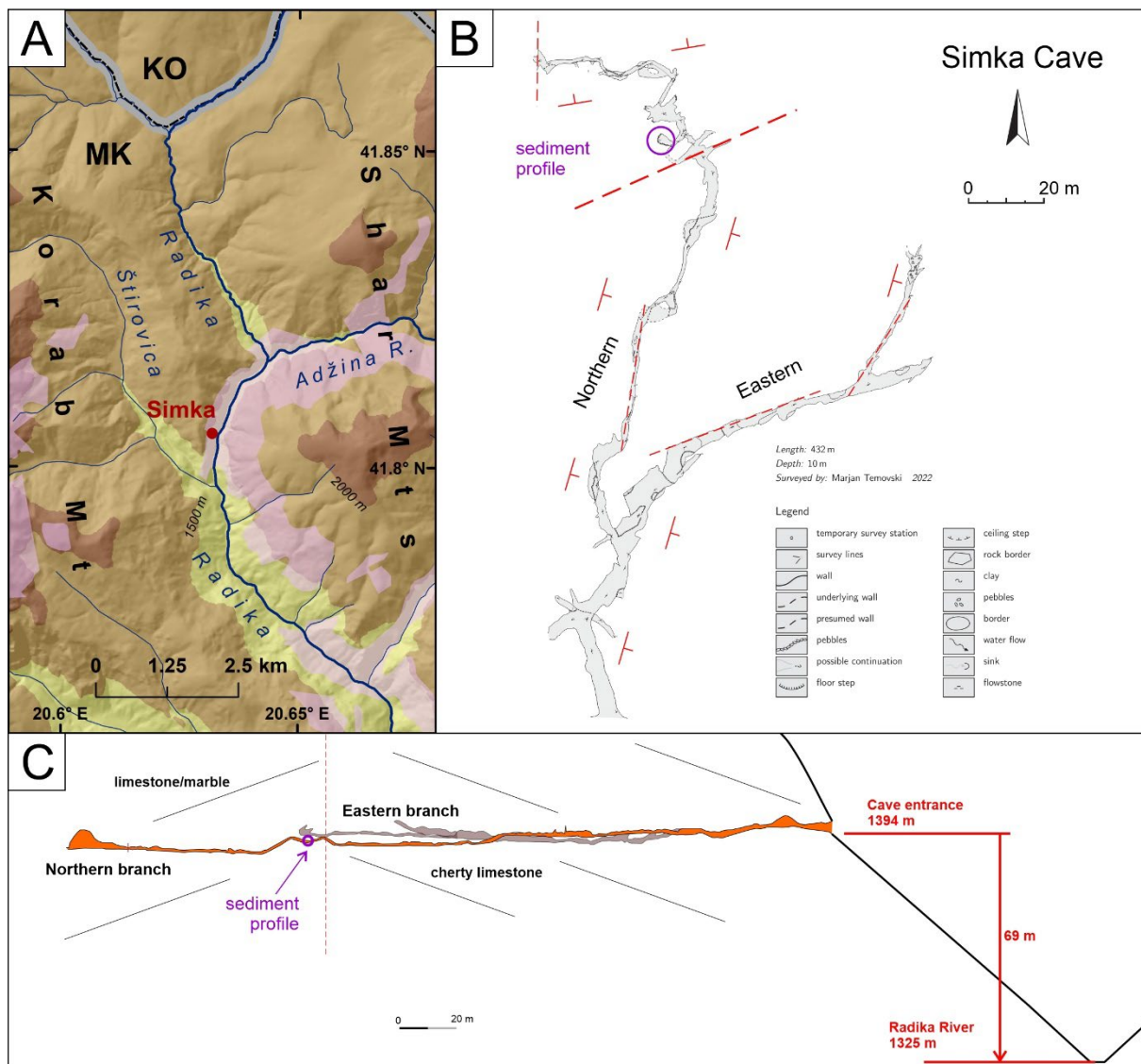


Fig. 18. Location (A) and map of Simka Cave in plan (B) and profile (C) view, showing location of the studied sediment profile and topographic relationship to Radika Valley. Surface extension of carbonate rocks in A is shown in pink shade.

Simka Cave has two main passages, an eastern and a northern branch, that diverge at about 50 meters from the entrance. Both branches are mainly strike- and dip-controlled separated by faults, and the northern, longer one appears as the main branch (Fig. 18). Clastic sediments, gravel and sand are found throughout the cave, except in the entrance part, where either they are completely eroded or covered by the ceiling rock breakdown material.

In the northern branch, upstream from the main fault line, a small side passage is completely choked with siliciclastic sediments; mostly allochthonous fluvial sand and gravel intercalated and topped by silty and clayey layers. The total height of the profile is 1.85 m (Fig. 19).

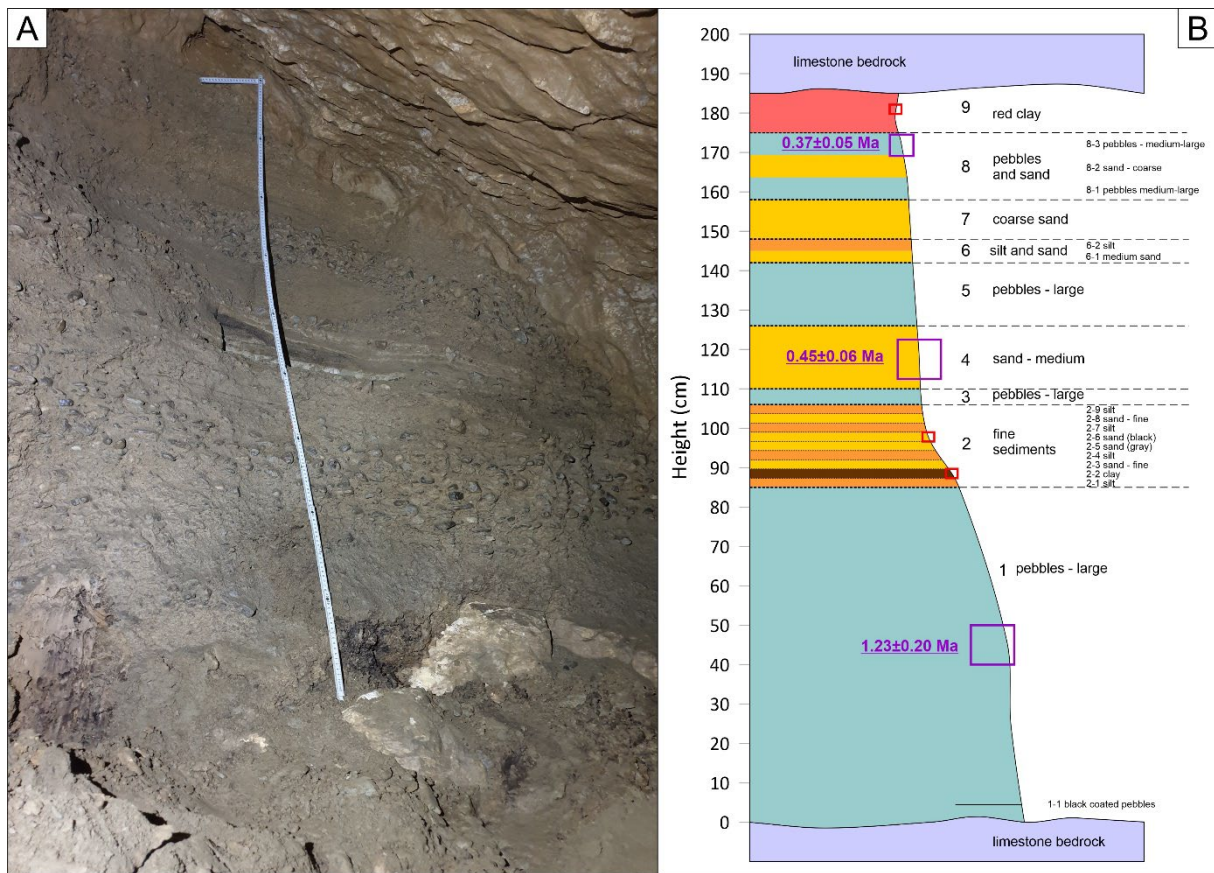


Fig. 19. View of the studied sedimentary profile (A) and the mapped stratigraphy with location of sampled layers and the obtained CRN burial ages

The coarser layers, indicative of channel facies, are generally covered by sands deposited by the stream of decreased flow. The finer layers (silt to clay) are slack-water deposits representing the end of flooding. The sediment profile shows several flooding episodes, with likely erosion of the upper part of the previous sequences. It finishes with a red clay cap, which probably represents the last flooding before the onset of incision.

The presence of high velocity flooding waters is indicated also by small size scallops found on cave walls. Furthermore, paragenetic ceiling morphology can be seen at the sampling profile and also along main passages in the Northern branch. These features indicate complete infilling of passages with sediments, that have been subsequently eroded. Based on the geometry of cave passages, it is very likely that the cave was fed by sinking water in the Štirovica valley, with possibly the Eastern branch being fed by water from an upstream location in Radika valley.

The CRN burial ages from the studied profile are in stratigraphic order. The  $1.23 \pm 0.20$  Ma CRN burial age of the lower, ~85 cm thick gravel layer, places the earliest cave development into the Early Pleistocene. This was followed by a hiatus that might include several phases of sedimentation and erosion. From the upper, more stratified part of the profile two samples were taken, which provided much younger, Middle Pleistocene ages: a medium sand layer ~30 cm above the top of the bottom gravels was deposited at  $0.45 \pm 0.06$  Ma and the last coarse sediments were deposited by the underground river at  $0.37 \pm 0.05$  Ma. After this last flooding event the cave was apparently abandoned by the incising river.

Considering this age and the current height of ~69 m of the cave above the riverbed, an incision rate of  $186^{+30}_{-22}$  m/Ma is estimated.

### 3. Methodologically connected studies

#### 3.1. Terrace chronology and quantification of the uplift of the TR

Aside of allocthonous sediments trapped in cave galleries at diverse height above the current riverbed, fluvial terraces are traditional geomorphological records for the quantification of river incision and surface uplift. Terrace ages deduced from diverse geochronological records yielded inconsistent data in the Danube valley in Hungary. To establish a more robust chronology, and hence to infer reliable incision/uplift rates, new CRN ages ( $^{10}\text{Be}$  depth profiles,  $^{26}\text{Al}/^{10}\text{Be}$  burial durations and burial depth profile) and luminescence-based ( $\text{pIRIR}_{290}$ ) terrace ages were acquired and compared to revised paleontological, published U/Th and magnetostratigraphic data. All the applied geo-chronometers led to concordant terrace ages, with the exception of the U/Th method applied on travertine deposits covering terraces. U/Th ages predating the last interglacial manifested a bias towards younger ages, and so they were ignored in relation to the quantification of terrace ages. As a result of the combination of diverse methodologies, terrace ages from the Late Pliocene to Late Pleistocene were settled. The modelling of cosmogenic  $^{26}\text{Al}$  and  $^{10}\text{Be}$  concentrations also enabled to derive surface denudation rates and helped to decide between diverse landscape evolution scenarios (Ruszkiczay-Rüdiger et al., 2018).

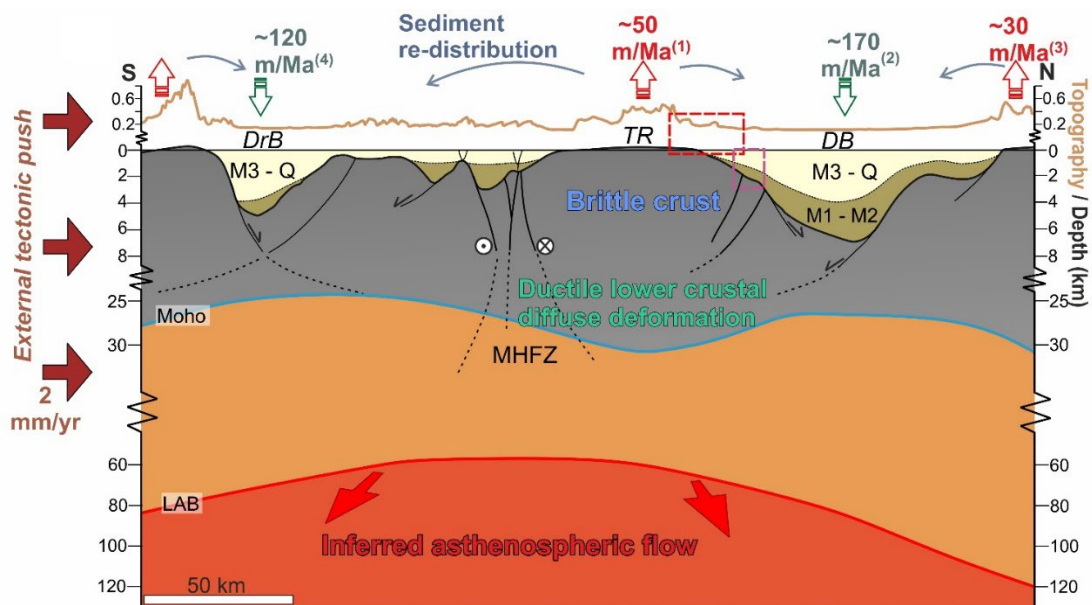


Fig. 20. Simplified lithospheric-scale cross-section over the western part of the Pannonian Basin. The section shows the main tectonic and surface processes that control the neotectonic phase of basin evolution. The model takes into account the increased intraplate stress governed by the northward push of the Adriatic microplate and associated induced gravitational stresses. It also considers the asthenosphere dynamics induced differential vertical movements facilitated by sediment re-distribution and associated lower crustal ductile deformation (Balázs et al., 2017). DrB – Dráva Basin, TR – Transdanubian Range, DB – Danube Basin. Large arrows in the asthenosphere indicate mantle flow oblique to the section. M1-M2: Lower- to Middle Miocene; M3-Q: Late Miocene to Quaternary. (1) This study, (2) Šujan et al. (2018); (3) Šujan et al. (2017); (4) Saftić et al. (2003) (Ruszkiczay-Rüdiger et al., 2020b).

By the synthesis of the previously acquired terrace chronological data, cumulative incision rates of  $\sim 50\text{--}70$  m/Ma integrating over the last  $\sim 3$  Ma have been derived for the Danube river cutting through the Transdanubian Range in the Western Pannonian Basin. An apparent acceleration of uplift rates was observed for shorter timescales culminating at  $\sim 200$  m/Ma over the last  $\sim 140$  ka. An examination of the change of the incision rates through time revealed that the incision rate was fairly constant at  $\sim 50$  m/Ma from  $\sim 3$  Ma to  $\sim 140$  ka, and the faster rates are valid only for the last  $\sim 140$  ka. These findings suggest that the long-term uplift rate

of the northwestern limb of the Transdanubian Range is  $\sim 50$  m/Ma, and the apparent acceleration of river incision during the Late Pleistocene is considered as the result of faster, most probably climate-driven incision during the last glacial cycle, outpacing the long-term uplift rate.

The study of seismic reflection profiles demonstrated that the observed upper crustal neotectonic faults are not sufficient to accommodate the deformation necessary for the reported Pliocene to Quaternary vertical motion. The geodynamic model for the explanation of the magnitude and pattern of surface uplift in the western Pannonian Basin involves a complex interplay between (1) deep lithosphere-asthenosphere dynamics, (2) structural inversion governed by the northward drift of Adria, (3) inherited geological structures and (4) climate driven surface processes (denudation and sediment loading) (Fig. 20) (Ruszkiczay-Rüdiger et al., 2020b).

These results help to understand the ongoing tectonic processes at the mountains surrounding the Pannonian Basin. The methodological achievements support a more robust approach in the study of the Plio-Quaternary uplift rates in the Central Balkan Peninsula as well.

### ***3.2. Laboratory intercomparison of sample processing procedures***

In the course of sample processing for CRN age determination throughout the project several technical issues raised that needed handling in order to produce robust exposure and burial ages. Most typical problems are the difficulties of the extraction of pure Al and Be targets or the loss of CRNs during the sample processing. These problems may lead to large age uncertainties and/or to biased apparent age data. Cosmogenic radionuclide  $^{10}\text{Be}$  and  $^{26}\text{Al}$  targets ( $\text{BeO}$  and  $\text{Al}_2\text{O}_3$ ) for AMS analysis are produced by a growing number of geochemical laboratories, employing different sample processing methods for the extraction of Be and Al from environmental materials. The reliability of this geochronological tool depends on data reproducibility independent from the preparation steps and the AMS measurements. The results of the laboratory intercomparison of sample processing protocols demonstrated that  $^{10}\text{Be}$  and  $^{26}\text{Al}$  concentrations of targets processed following different, commonly used protocols and measured at two AMS facilities lead to consistent results. However, the study also demonstrated that insoluble fluoride precipitates may form during evaporation of certain samples, mostly those that appear to be difficult in obtaining pure quartz separates. The study revealed that the formation of insoluble fluoride precipitates leave  $^{10}\text{Be}$  concentrations unaffected, but can cause decreased  $^{26}\text{Al}$  concentrations, leading to considerably older apparent burial durations compared to the real burial time of the sample. As a result, thorough cleaning of the quartz and an improved sample processing protocol are suggested to avoid fluoride precipitate formation (Ruszkiczay-Rüdiger et al, 2021b). The analysed sample set originated from a terrace of the Danube River in the Vienna Basin, targeting the age determination of the terrace level and quantification of the incision/uplift rates at the Vienna Basin as well. This research was also supported by two small projects of the Austro-Hungarian Action Foundation (OMAA 90öu17 and OMAA 98öu17).

**SUBMITTED, UNDER REVISION**

### ***3.3. CRN burial age determination with advanced outlier identification and comparison of different burial dating models***

The comparison and improvement of the laboratory procedures of CRN extraction chemistry is followed by the comparison of different burial age calculation models and elaboration of a routine for robust outlier selection. In this study two published CRN  $^{26}\text{Al}/^{10}\text{Be}$  burial age calculation methods, developed to correct for post-depositional production of nuclides in settings with shallow sediment overburden are compared. The advantages and limitations of isochron burial dating (ISO) and inversion modelling burial dating (INV) are investigated on a dataset from two depth levels of a 14 m thick sandy gravel sediment of a terrace of the Danube River located in the Central Vienna Basin (Austria) with CRN concentrations published by Ruszkiczay-Rüdiger et al. (2012b). This research was also supported by two small projects of the Austro-Hungarian Action Foundation (OMAA 90öu17 and OMAA 98öu17).

The robustness of the results was verified by several steps of outlier identification, starting from the traditional way of examining the sample position with respect to the isochron line. This was combined with novel methods of

bootstrapping and testing the ratio of post-burial and measured CRN inventories. Outlier identification and age determination were run iteratively until converging to the best estimate model solutions.

The two methods provided ages in good agreement at  $1.2 \pm 0.4$  Ma for both quarry levels only if outliers were recognized and excluded, considered as the most probable burial age of the terrace. The sink denudation rate determined using INV for the upper level ( $16.1 \pm 11.7$  m/Ma) was higher than that for the lower level ( $6.3 \pm 3.7$  m/Ma), however in agreement within uncertainties. This might indicate a mean denudation rate of  $11.6 \pm 9.0$  m/Ma, or a recent change of the surface denudation rate.

The INV model was run with the data from the two levels merged ( $n=11$ ) to test outlier sensitivity of the method in case of a larger dataset. These results suggest that a larger dataset is less sensitive to the presence of outliers, however, identification of outliers is still recommended.

## 4. Final remarks, work in progress and future plans

### 4.1. Work in progress

As it was described in the previous sections, large amount of data from the present project is still under evaluation, and at least four peer reviewed papers are expected to be submitted on their basis.

The laboratory inter-comparison project made obvious that there was a need for an easy and objective way to control the purity of quartz separates for CRN dating. For this purpose a small project was launched in cooperation with the Luminescence and Cosmogenic Nuclide laboratories of the BOKU (Vienna) and with the Luminescence laboratory of the Eötvös Univeristy (Budapest). The first results were presented on conferences.

Besides, a preliminary investigation of caves in Hungary (Pilis, Mecsek – also supported by the RHK) has also started by field visits searching for allochthonous quartz-rich sediments suitable for burial age determination and quantification of uplift rates. Some preliminary samples were already taken, these are in different stages of sample processing, AMS measurement and data evaluation. The first results were presented on conferences.

In search of suitable sample locations the formerly glaciated and highly karstified Lovćen Mt, near the Adriatic coast in Montenegro was also visited with twofold aims. First was the search of deep caves with allochthonous, datable sediments to quantify uplift rates. Unfortunately, no suitable cave sediments could be found. At the higher, cirque area of the same range glacial sediments were also studied in search of suitable material for an attempt of the application of CRN  $^{36}\text{Cl}$  on the limestone lithologies. However, the dissolution features on the moraine boulders suggested high and variable surface denudation rates, rendering them most probably unsuitable for proper CRN dating. Further locations are in search for both the quantification of uplift rates in the region and for the comparison and verification of the  $^{36}\text{Cl}$  and  $^{10}\text{Be}$  CRE dating methods.

### 4.2. Continuation and extension of the started work

Partly based on the achievements of the present project, and as a continuation and extension of the geomorphological and geochronological work on glaciations and quantification of uplift rates in the region, a project proposal entitled *Climate- and tectonics-related surface processes in the Southern Carpathians and Northern Balkan Mountains. A geochronological approach at different timescales (ChronoCaRP)* was submitted to the call of Romania's National Recovery and Resilience Plan (PNRR) with the leadership of Zsófia Ruzsiczay-Rüdiger. The proposed research plan got support, and the 3 years grant has already launched in July 2023 (<https://chronocarp.unibuc.ro/> - website under construction). The research aims at a better understanding of the relationship between climate oscillations and Quaternary landscape evolution in SE Europe. The targeted areas are the formerly glaciated mountains of the Southern Carpathians in Romania (Retezat, Fagaras, Bucegi Mts) and Rodope Massif in Bulgaria (Rila and Pirin Mts). Besides the terraces of the Danube River at the Iron Gates will be studied for a revised terrace stratigraphy and in order to provide new terrace chronological data (OSL and CRN) and novel incision/uplift rates.

## References

- Arsovski, M. (1997): Tektonika na Makedonija. Rudarsko-geološki fakultet, Štip, 360 p. (in Macedonian)
- Andonovski T., 1984. Pešteri vo gorniot tek od dolinata na Radika – Torbeški Most, Zbornik Predavanja, Deveti Jugoslavenski Speleoloski Kongres, Zagreb, 293-299 (in Macedonian).
- Balázs, A., Burov, E., Maženco, L., Vogt, K., Francois, T., Cloetingh, S., 2017. Symmetry during the syn- and post-rift evolution of extensional back-arc basins: the role of inherited orogenic structures. *Earth Planet. Sci. Lett.* 462, 86–98.
- Dumurdžanov, N., Serafimovski, T., Burchfiel, B.C., 2004. Evolution of the Neogene-Pleistocene basins of Macedonia. *Geol Soc Am Digit Map Chart Ser 1*, 1–20.
- Dumurdžanov, N., Serafimovski, T., Burchfiel, B.C. (2005): Cenozoic tectonics of Macedonia and its relation to the South Balkan extensional regime. *Geosphere*, 1, 1–22.
- Kuhlemann, J., Milivojevic, M., Krumrei, I., Kubik, P.W., 2009. Last glaciation of the Sara range (Balkan peninsula): Increasing dryness from the LGM to the Holocene. *Austrian J. Earth Sci.* 102, 146–158.
- Lilienberg, D.A., 1968. The main regularities in recent movements in the central parts of the Balkan peninsula (on the example of Macedonia). *Studia Geophys. et Geodaetica* 12, 163–178.
- Menković, L., Milivojević, M. 2021. Glacial Morphology of the Sara Mountains. *Bull. of the Serbian Geographical Societs*, 101(1), 1-29.
- Milevski, I., Gorin, S., Markoski, M., Radevski, I., 2013. Comparison of Accuracy of DEM's Available for the Republic of Macedonia. *Proceedings from the 3<sup>rd</sup> International Geographic Symposium - GEOMED 2013, Antalya*, 165–172.
- Milevski, I., Temovski, M., Madarász, B., Kern, Z., & Ruszkiczay-Rüdiger, Z. (2020). Geomorphometry of the cirques of Shar Mountain. *Geomorphometry*, S. 91-94.
- Osmaston, H., 2005. Estimates of glacier equilibrium line altitudes by the Area×Altitude, the Area×Altitude Balance Ratio and the Area×Altitude Balance Index methods and their validation. *Quat. Int.* 138–139, 22–31.
- Pavićević, M. K., Cvetković V., Niedermann, S., Pejović V., Amthauer G., Boev B., Bosch F., Aničin I., Henning W. F., 2016. Erosion rate study at the Allchar deposit (Macedonia) based on radioactive and stable cosmogenic nuclides (<sup>26</sup>Al, <sup>36</sup>Cl, <sup>3</sup>He, and <sup>21</sup>Ne). *Geochemistry, Geophysics, Geosystems*, 17, 410–424.
- Pellitero, R., Rea, B.R., Spagnolo, M., Bakke, J., Hughes, P., Ivy-Ochs, S., Lukas, S., Ribolini, A., 2015. A GIS tool for automatic calculation of glacier equilibrium-line altitudes. *Comput. Geosci.* 82, 55–62.
- Pellitero, R., Rea, B.R., Spagnolo, M., Bakke, J., Ivy-Ochs, S., Frew, C.R., Hughes, P., Ribolini, A., Lukas, S., Renssen, H., 2016. GlaRe, a GIS tool to reconstruct the 3D surface of palaeoglaciers. *Comput. Geosci.* 94, 77–85.
- Ruszkiczay-Rüdiger, Zs., Csillag, G., Fodor, L., Braucher, R., Novothny, Á., Thamó-Bozsó, E., Virág, A., Pazonyi, P., Timár, G., ASTER Team 2018. Integration of new and revised chronological data to constrain the terrace evolution of the Danube River (Gerecse Hills, Pannonian Basin). *Quaternary Geochronology* 48.
- Ruszkiczay-Rüdiger, Zs., Kern, Z., Temovski, M., Madarász, B., Milevski, I., Braucher, R., ASTER Team, 2020a. Last deglaciation in the central Balkan Peninsula: Geochronological evidence from Jablanica Mt. (North Macedonia). *Geomorphology* 351, 106985.
- Ruszkiczay-Rüdiger, Z., Balázs, A., Csillag, G., Drijkoningen, G., & Fodor, L. 2020b. Uplift of the Transdanubian Range, Pannonian Basin: How fast and why? *Global and Planetary Change*, 103263. 1-17.
- Ruszkiczay-Rüdiger, Z., Kern, Z., Urdea, P., Madarász, B., Braucher, R., ASTER Team, 2021a. Limited glacial erosion during the last glaciation in mid-latitude cirques (Retezat Mts, Southern Carpathians, Romania). *Geomorphology* 384, 107719.
- Ruszkiczay-Rüdiger, Zs., Neuhuber, S., Braucher, R., Lachner, J., Steier, P., Wieser, A., Braun, M., ASTER Team, 2021b. Comparison and performance of two cosmogenic nuclide sample preparation procedures of in situ produced <sup>10</sup>Be and <sup>26</sup>Al. *J. Radioanal. Nucl. Chem.* 329, 1523–1536.
- Ruszkiczay-Rüdiger, Zs., Temovski, M., Kern, Z., Madarász, B., Milevski, I., Lachner, J., Steier, P. 2022. Late Pleistocene glacial advances, equilibrium-line altitude changes and paleoclimate in the Jakupica Mts (North Macedonia). *CATENA*, 216, 106383.



- Ruszkiczay-Rüdiger, Zs., Neuhuber, S., Hintersberger, R., Nørgaard, J., Braucher, R. (in revision). Advanced outlier identification of cosmogenic radionuclide data and comparison of different approaches of burial dating tested on a fluvial terrace in the Vienna Basin. *Quaternary Geochronology*.
- Serpelloni, E., Cavaliere, A., Martelli, L., Pintori, F., Anderlini, L., Borghi, A., Randazzo, D., Bruni, S., Devoti, R., Perfetti P., and Cacciaguerra S., 2022. Surface Velocities and Strain-Rates in the Euro-Mediterranean Region from Massive GPS Data Processing. *Front. Earth Sci.* 10, 907897.
- Saftić, B., Velic, J., Sztanó, O., Juhász, Gy, Ivkovic, Z., 2003. Tertiary subsurface facies, source rocks and hydrocarbon reservoirs in the SW part of the Pannonian Basin (Northern Croatia and South-Western Hungary). *Geol. Croatica* 56, 101–122.
- Šujan, M., Lačný, A., Braucher, R., Magdolen, P., ASTER Team 2017. Early Pleistocene age of fluvial sediment in the Stará Garda Cave revealed by  $^{26}\text{Al}/^{10}\text{Be}$  burial dating: implications for geomorphic evolution of the Malé Karpaty Mts. (Western Carpathians). *Acta Carsologica* 46/2, 251-264.
- Šujan, M., Braucher, R., Rybár, S., Maglay, J., Nagy, A., Fordinál, K., Šarinová, K., Sýkora, M., Józsa, S., Kovač, M., ASTER Team, 2018. Revealing the late Pliocene to Middle Pleistocene alluvial archive in the confluence of the Western Carpathian and Eastern Alpine rivers:  $^{26}\text{Al}/^{10}\text{Be}$  burial dating from the Danube Basin (Slovakia). *Sedimentary Geology*, 377. 131-146.
- Temovski, M., 2016. Evolution of karst in the lower part of Crna Reka river basin. Springer Theses, Springer International Publishing, 265 p.
- Temovski M., Audra Ph., Mihevc A., Spangenberg J., Polyak V., McIntosh W., Bigot J-Y. (2013): Hypogenic origin of Provalata Cave, Republic of Macedonia: a distinct case of successive thermal carbonic and sulfuric acid speleogenesis. *International Journal of Speleology*, 42 (3), 235-246.
- Temovski, M., Madarász, B., Kern, Z., Milevski, I., Ruszkiczay-Rüdiger, Zs., 2018. Glacial Geomorphology and Preliminary Glacier Reconstruction in the Jablanica Mountain, Macedonia, Central Balkan Peninsula. *Geosci.* 8, 1–21.
- Temovski M., Rinyu L., Futó I., Palcsu L., 2022a. Some insight on hydrothermal speleogenesis based on conventional and clumped carbonate stable isotopes – preliminary results from the Mariovo hypogene karst system. In: Gauchon C., Jaillet S., *Proceedings of the 18th International Congress of Speleology*, vol IV, 189-192.
- Temovski M., Rinyu L., Futó I., Molnár K., Túri M., Demény A., Otoničar B., Dublyansky Y., Audra P., Polyak V., Asmerom Y., Palcsu L., 2022b. Combined use of conventional and clumped carbonate stable isotopes to identify hydrothermal isotopic alteration in cave walls. *Scientific Reports* 12, 9202.
- Temovski, M., Wieser, A, Marchart, O., Braun, M., Madarász, B., Kiss, G.I., Palcsu, L., Ruszkiczay-Rüdiger, Zs. 2023. Pleistocene valley incision, landscape evolution and inferred tectonic uplift in the central parts of the Balkan Peninsula – insight from geochronology of cave deposits in the lower part of Crna Reka basin (N. Macedonia), *Geomorphology*, (in revision)
- Tîrlă, L., Drăgușin, V., Bajo, P., Covaliov, S., Cruceru, N., Ersek, V., Hanganu, D., Hellstrom, J., Hoffmann, D., Mirea, I., Sava, T., Sava, G., Șandric, I., 2020. Quaternary environmental evolution in the South Carpathians reconstructed from glaciokarst geomorphology and sedimentary archives. *Geomorphology*, 354, 107038.